Regulation of RAW264.7 Macrophage Polarization on Smooth and Rough Surface Topographies by Galectin-3

by

Fariba Kianoush

BSc 2009

Ferdowsi University of Mashhad

A THESIS SUBMITTED IN PARTIAL FULFILLMENT OF

THE REQUIREMENTS FOR THE DEGREE OF

MASTER OF SCIENCE

in

THE FACULTY OF GRADUATE AND POSTDOCTORAL STUDIES

(Craniofacial Science)

THE UNIVERSITY OF BRITISH COLUMBIA

(Vancouver)

November 2015

Abstract

Surface topography can modulate cytokine gene expression and protein secretion in macrophages. Although phosphoinositide 3-kinase (PI3K) has been found to have a key role in the induction of the alternatively activated phenotype (M2) by interleukin 4 (IL-4), the pathways involved in topographic modulation of phenotype are largely unknown. This study examined the effect of polished (PO) and three rough surfaces, SLA (Sandblasted Large-grit Acid-etched surface which is a well-documented and widely used implant surface) and two novel grooved topographies G1 and G2 produced by anisotropic etching of Si <110> for their effects on RAW 264.7 macrophage gene expression and morphology using real time quantitative polymerase chain reaction (RT-qPCR). We hypothesized that the galectin-3/ CD98/ integrin β1 complex was involved in phenotype regulation. The hypothesis was tested by blocking attachment of galectin-3 (gal-3) to CD98 by lactose. The G1 and G2 surfaces caused the macrophages to adopt an elongated M2-like morphology. In the presence of lactose the M2 markers were downregulated but the M1 marker was upregulated on smooth and rough surfaces. Thus the inhibition of gal-3 binding to integrin skewed macrophages phenotype towards the M1 phenotype and the effects of topography were thus abrogated. To test if PI3K is involved in regulation of macrophage phenotype on rough and smooth topographies (without any exogenously added IL-4/IL-13), we studied the effects of the PI3K inhibitor, LY294002, on phenotype markers. As expected from the results with IL-4 induced polarization, an M2 marker (the mannose receptor) was downregulated on both PO and G1 surfaces. Our data suggest that galectin-3 dependent CD98 interaction with integrin β1 skewed RAW264.7 cells toward an M2-like phenotype on both smooth and rough surface topographies through CD98-activated PI3K. Furthermore, we report

that rough surface topography plays a substantive role in directing macrophages towards the M2 phenotype. This was reflected in both M2 marker expression and cellular morphology.

Preface

This dissertation is the original work of the author, Fariba Kianoush and several collaborators:

- The identification and design of the project reported in this thesis was conceived by D.M. Brunette, J.D. Waterfield and Mandana Nematollahi
- Reproduction of surface topographies in epoxy, RAW264.7 macrophage cell culturing, RNA extraction and purification, RNA quality analysis, Real Time Quantitative Polymerase Chain Reaction (RT-qPCR) and analysis of RT-qPCR in Microsoft Excel, staining samples for immune fluorescent microscopy, cytokine microarray and ELISA in Chapter 3 were performed by F. Kianoush
- Preparing samples for Scanning Electron Microscopy (SEM) and analysis of the images for cell elongation study were performed by F. Kianoush (50%) and H. Moon (50%)
- Confocal Microscopy and Scanning Electron Microscopy was performed at UBC Centre of High-Throughput Phenogenomics by F. Kianoush (20%) and Q. Ho (80%)
- All the statistical analyses mentioned in this thesis were performed by F. Kianoush
- The hypothetical model in Chapter 5 was illustrated by F. Kianoush
- G1 and G2 surface characterization was performed by Dr. CVM Cremmel in the laboratory of Dr. N.D. Spencer (Swiss Federal Institute of Technology, Zurich)

Material in this thesis was presented at the 2014 Canadian Society of Biomaterials meeting in Halifax, Nova Scotia.

Table of Contents

List of Tables

List of Figures

List of Abbreviations

2D	2 dimension
3D	3 dimension
Arg-1	Arginase-1, catalyzes arginine hydrolysis to urea and ornithine, a known M2 phenotype marker in macrophages
BSA	Bovine Serum Albumin
CCL2	C-C ligand 2 chemokine Also known as MCP-1, monocyte chemotactic protein-1
CCL3	C-C ligand 3 chemokine Also known as MIP-1α, macrophage inflammatory protein 1 alpha
CCL4	C-C ligand 4 chemokine Also known as MIP-1β, macrophage inflammatory protein 1 beta
CCL7	C-C ligand 7 chemokine Also known as MCP-3, monocyte chemotactic protein 3
CD98	Galectin-3 receptor on macrophage membrane
cDNA	Complementary DNA
cpTi	Commercially pure Titanium
DAPI	4',6-diamidino-2-phenylindole, fluorescent dye binding to DNA
DMSO	Dimethyl sulfoxide, dissolves both polar and non-polar solvents
ERK	Extracellular signal-regulated kinase
FAK	Focal adhesion kinase
G1	Grooved-1
G2	Grooved-2
Gal-3	Galectin-3
IFN-γ	Interferon gamma

IL-1	Interleukin-1
IL-13	Interleukin-13
IL-4	Interleukin-4
IL-6	Interleukin-6
iNOS	Inducible nitric oxide synthase
IP-10	Interferon gamma-induced protein 10
LPS	Lipopolysaccharide
M1	Classically activated macrophages
M2	Alternatively activated macrophages
mM	Milli molar
nM	Nano molar
MCP-1	Monocyte chemotactic protein-1, also known as CCL2
MCP-3	Monocyte chemotactic protein-3, also known as CCL7
MIP-1β	Macrophage inflammatory protein-1 beta, also known as CCL4
mm	Millimeter
nm	Nano meter
ml	Milliliter
um	Micro molar
MR	Mannose receptor, a lectin on macrophage membrane which is involved in the resolution of inflammation, a known M2 marker
NFkB	Nuclear factor kappa-light-chain-enhancer of activated B cells
nRTC	No reverse transcriptase control
NTC	No template control

PI3K	Phosphoinositide 3-kinases
PO	Polished
Ra	Average roughness over all points on a profile
Sa	Average roughness over all points on a surface
Si	Silicon
SLA	Sandblasted, large-grit, acid-etched

Acknowledgements

I would like to thank my knowledgeable supervisor, Dr. D. M. Brunette for his advices, support, guidance and patience. It was an honor to have the opportunity to work with him and learn from him.

I would like to thank my knowledgeable co-supervisor, Dr. J.D. Waterfield for all his help and guidance throughout my study.

I also thank my dear committee members, Dr. Clive Roberts and Dr. E. Putnins for their great advices throughout my study.

I am thankful for the members of the Brunette lab for their support and help. I would like to specially thank my amazing colleagues and friends Ms. Haisle Moon and Ms Quan Ho for all the help and support.

I appreciate kindness of Dr. C. Shuler lab for allowing me to use their nanodrop spectrophotometer and PCR machine and the Dr. E. Putnins lab for allowing shared use of the ultrasonic machine, mastercycler, centrifuge, and scanner.

I also would like to thank Dr. N.D. Spencer from Swiss Federal Institute of Technology Zurich for all his help. I give many thanks to Dr. C.V.M Cremmel for the characterization of the novel grooved surfaces. I would like to thank Dr. A. Kulpa and Dr. N.A.F. Jaeger for the fabrication of the novel grooved surfaces.

Dedication

I dedicate this thesis to my parents for their unconditional love and support.

I dedicate this thesis to my love, husband and friend, Alireza for all his love and support.

I dedicate this thesis to my amazing brothers, Kamyar and Kasra.

Chapter 1: Introduction

1.1 A General Introduction to Macrophages

The evolution of our understanding of macrophage function from their role as simple non-specific phagocytic cells ("garbage men of the body" (Nathan 2012)) to cells regulating non-specific and specific immune responses has resulted in remarkable advances in our ability to manipulate immune function. The human immune system comprises two main sub systems; the non-specific (innate) and specific immune system (Abbas et al. 2014). Peripheral blood mononuclear cells (PBMCs) are precursors for the innate immune system cells including basophils, eosinophils and monocytes (Mosser & Edwards 2008). During the steady state as well as inflammation, these cells migrate from the blood stream into tissues (Mosser & Edwards 2008). Monocytes eventually differentiate into resident macrophages (Abbas et al. 2014), the main differentiated cells of the mononuclear phagocyte system (Russell 1992), present in almost all tissues. Both the innate and specific immune responses are initiated when macrophages recognize pathogens and phagocytize them. To produce an effective immune response, macrophages recognize pathogen-associated molecular patterns (PAMPs) using pattern recognition receptors on their cell surface.

Binding of ligands to their various receptors cue the macrophage to initiate appropriate innate responses (Abbas et al. 2014). There are three main groups of receptors in macrophages: 1) receptors recognizing inflammatory cytokines and chemokines 2) pattern recognition receptors that mediate unregulated or regulated uptake of danger signals 3) integrin receptors (Gordon 2003).

Cytokine receptors transduce signals to the nucleus through a series of signaling intermediates. These receptors function in the control of cytokine/ chemokine production and determination of

macrophage phenotype. Toll-like receptors (TLRs) are a member of the cell-based pattern recognition receptors (PRRs) family that activate pro-inflammatory signaling pathways (Akira et al. 2001). TLR2 recognizes fungal and mycobacterial components while lipopolysaccharide (LPS) is recognized by TLR4 (Ozinsky et al. 2000). Other members of the toll family recognize mycoplasmas, DNA viruses and RNA viruses (Xagorari & Chlichlia 2008). Mannose receptor (MR) is a PRR that stimulates phagocytic responses and regulates resolution of inflammation in macrophages by recognizing and removing glycoproteins such as lysosomal hydrolyses (Linehan et al. 2000; Lee et al. 2002) MR expression is downregulated by proinflammatory molecules like LPS and interferon-γ in the beginning of the inflammatory responses, while in the resolution phase, MR expression gets upregulated (Lee et al. 2002).

1.1.1 Macrophage Plasticity

Macrophage morphology changes in response to early endogenous stimuli produced by damaged tissue cells or innate immune system components following injury or infection. Antigen-specific immune cells and macrophages themselves are also capable of producing signals altering macrophage physiology (Gordon 2007; Mosser & Edwards 2008). Exposure of macrophages to a variety of external stimuli (cytokines, bacterial products, growth factors and chemotactic cytokines/ chemokines) induces two distinct pathways of activation and polarized phenotype: M1and M2 (Mantovani et al. 2002; Munder et al. 1998; Goerdt et al. 1999). Classically activated (M1) macrophages mediate protective immunity through interferon gamma (IFN-γ) activation in response to pathogens (Holscher et al. 2001; Mosser 2003). Alternatively activated macrophages or M2, function to suppress excessive inflammation and promote healing responses (Gordon 2003). Macrophages are not strictly confined to one phenotype and they can exhibit

characteristics of both M1 and M2 phenotypes. Their phenotype can then lie within a spectrum between the M1 and M2 phenotypes (Mosser & Edwards 2008; Sica & Mantovani 2012)

1.1.1.1 Classically Activated Macrophages

Classically activated (M1) macrophages are produced in response to damaged tissue or priming cells with bacterial lipopolysaccharide (LPS) as well as the combination of IFN-γ and tumor-necrosis factor (TNF). These classically activated macrophages are essential parts of host defense, producing proinflammatory mediators such as NOS2, IL-12 and IL-23 (O'Shea & Murray 2008). Since M1 macrophages play a key role in mediating immunopathology during autoimmune disease, their activity must be controlled (Zhang & Mosser 2008; Szekanecz & Koch 2007). Secreted molecules defining the M1 phenotype (M1 markers) include cytokines such as IL-1, IL-6, IL-23, the chemokine CXCL-10 (IP-10) and the enzyme, NOS2 (which oxidizes the terminal guanidine group of L-arginine to produce nitric oxide (NO) (Bogdan 2001). The M1 markers are also associated with the expansion of TH 17 cells, which produce IL-17, IL-21 and IL-22 (Mosser & Edwards 2008; Mantovani et al. 2004).

As the signaling pathway involved, the toll like receptors (TLR) as well as the IL-1 receptors use the universal adaptor protein MYD88 and TRAF6 to activate proinflammatory cytokines through the nuclear factor kappa-light-chain-enhancer of activated B cells (NF-kB) and mitogen-activated protein kinase (MAPK) pathway. In contrast, IFNγ and IL-6 use the Janus kinase family (JAK)/ signal transducer and activator of transcription pathway (STAT) to activate the proinflammatory phenotype. It has also been shown that JAK/STAT pathway regulates polymerization and stabilization of microtubules (Nicolas et al. 2012; Groner & Hennighausen

2012). Goldman (1971) found that microtubule organization affects the cell shape and cell spreading of fibroblasts.

1.1.1.2 Alternatively Activated Macrophages

Alternatively activated macrophages also develop in response to innate or adaptive signals. Macrophages primed with IL-4/ IL-13 are known as M2 or alternatively activated macrophages and are involved in wound healing process at the injury site. IL-4 and IL-13 are produced in allergic or immune responses to parasites and pathogens and they induce macrophages to become elongated. IL-4 is one of the first signals to be released during tissue injury (Loke et al. 2002). Although there are different types of cells contributing to IL-4 production, two important sources for IL-4 secretion are mast cells and basophils (Brandt et al. 2000). IL-4 stimulates arginase-1, which converts L-arginine to ornithine, a precursor of polyamines and collagen and consequently contributes to the production of the extracellular matrix and wound healing (Kreider et al. 2007).

Alternatively activating macrophage upregulates the expression of mannose receptor (MR), which is a lectin located on the macrophages surfaces (Stein et al. 1992) and it is used as a marker for the M2 phenotype (Gordon 2003; Mantovani et al. 2004). Similar to M1 markers, there are also chemokines (CCL-2 (MCP-1)), cytokines (IL-10), enzymes (arginase-1), proteins (FIZZ1) and lectins (Ym-1), which are considered as M2 markers (Gordon 2003). The M2 inducer molecule, IL-4, is recognized by the membrane receptor IL-4Rα (Nelms et al. 1999). The IL-4Rα chain binds IL-4 with high affinity (Moy et al. 2001), leading to dimerization with a second chain, gamma common (γc) chain (Nelms et al. 1999). This dimerization induces a cytoplasmic signaling cascade that involves the JAK family (Keegan et al. 1995; Leonard &

Shea 1998), the insulin receptor substrate family (Kelly-welch et al. 2003), and the phosphoinositide 3-kinase (PI3K) pathway. Activation of M1 cells temporarily blocks activation of M2 cells through suppression of cytokine signaling3 (SOCS3) and conversely, activation of M2 cells temporarily blocks activation of M1 cells through production of SOCS1 (Wilson 2014). A list of M1 and M2 markers (Gordon 2003; Martinez & Gordon 2014) is given in Table 1-1.

Macrophages phenotype	Main inducers	Markers	Description
M2	IL-4, IL-13	MR	Mannose receptor
		Arginase 1	Counteracts NOS2 Expression induced by IFNγ/LPS
		IL-1, IL-6	Counteracts LPS-induced pro-inflammatory effect
		IL-10	Effects vary depending on timing of LPS stimulus. Promotes Th2 differentiation
		Ym1	Closely related soluble chitinase-like lectin. Expression controlled by IL-4/ INFγ in an antagonistic manner
		FIZZ1	Resistin-like secreted protein. Expression controlled by IL-4/ INFγ in an antagonistic manner
M1	LPS, INFγ	iNOS	Produce NO for intracellular killing
		CXCL9, 10, 11	Th1 chemokines
		TNFα	Tumor necrosis factor alpha
		COX-2	Cyclooxygenase, produces prostaglandins
		IL-1β	Interleukin 1 beta, proinflammatory cytokine
		IL-12	Interleukin 12, proinflammatory cytokine, promotes Th1 differentiation
		IL-6, IL-23	Proinflammatory cytokine

Table 1-1 List of M1 and M2 markers in macrophages

1.1.2 Galectin-3 and Its Function in Macrophages

Galectin-3 (Gal-3), a 30kDa lectin (sugar binding protein), is a chimeric protein that is highly expressed in macrophages (MacKinnon et al. 2008; Liu et al. 1995). It can adopt a proinflammatory role in acute tissue injury or play a wound healing role in chronic inflammation (Henderson & Sethi 2009). It binds to its membrane receptor CD98 facilitating its association with integrin β1 and upregulating PI3K activity (MacKinnon et al. 2008). In our study we used lactose (50mM) to block gal-3 function and gene expression of the phenotypic markers using iNOS as the M1 marker and mannose receptor as the M2 marker. Gal-3 is involved in different mechanisms such as cell growth, cell cycle and apoptosis. It has been shown that galectin-3 is a regulator of cell apoptosis as Yang et al. (1996) observed a higher apoptosis rate among the human leukemia cells that were not expressing gal-3 compared to the control group.

CD98 (125-kDa) is a heterodimeric transmembrane glycoprotein consisting a glycosylated heavy chain (85-kDa) and a non-glycosylated light chain (40-kDa). CD98 is expressed on macrophages and is known as galectin-3 receptor on the macrophage membrane (Dong & Hughes 1997). Henderson and Sethi (Henderson & Sethi 2009) have previously shown that CD98 physically associates with certain integrin β subunit (β1) cytoplasmic domains via its heavy chain. This association in turn stimulates an integrin-mediated increase in focal adhesion kinase (FAK) and PI3K activation. Henderson and Sethi (2009) found that alternative macrophage activation with IL-4 and IL-13 stimulated expression and release of galectin-3. By contrast, classical macrophage activation with IFNγ / LPS reduced expression of galectin-3. Therefore specific targeting of the galectin-3/CD98/PI3K pathway with inhibitors such as lactose may represent a novel therapeutic method for manipulating macrophage phenotype in the treatment of chronic inflammation, tissue fibrogenesis and cancer. Sica et al. stated that tumor associated

macrophages (TAM) are recruited to the site of the tumor by CCL-2/ MCP-1. They also mentioned that M1 macrophages are involved in the tumor suppression while M2 macrophages promote the tumor progression (Sica et al. 2006).

To further investigate the role of galectin-3, we also measured gene expression of pro and anti-inflammatory chemokines including MCP1/CCL2, CCL3/MIP1α, CCL4/MIP1β and CCL7/MCP3 on PO, SLA, G1 and G2 surfaces in the presence of lactose. CCL2 or monocyte chemoattractant protein 1 (MCP-1) recruits monocytes and macrophages to the inflammation site (Satish et al. 2009). CCL3 or macrophage inflammatory protein 1α (MIP-1α), CCL4 or macrophage inflammatory protein 1β (MIP-1β) and CCL7 or monocyte specific chemokine 3 (MCP3) are chemoattractants that attract monocytes and natural killer cells (Thompson & Van Eldik 2009; Bystry et al. 2001; Montecucco et al. 2008).

1.1.3 Integrins

Integrins are heterodimeric transmembrane proteins consisting of a combination of an alpha (α) and a beta (β) subunit that are involved in cell adhesion and also serve as signaling receptors (Rintoul et al. 2002). Intracellular signaling responses, which are produced by integrin clustering at the cell surface result in the actin cytoskeleton rearrangement and also adhesion and spreading of the cells (Meng & Lowell 1998). The Src family kinases are also thought to be involved in integrin-mediated cell adhesion and migration (Berton et al. 1994). Integrins are capable of regulating adhesion of cells to the extracellular matrix (ECM) proteins. Integrin α and β chains interact with ECM proteins and integrin ligands to become activated. This activation can affect cell apoptosis, differentiation, survival, proliferation, elongation, adhesion and migration by differentially activating a receptor-associated multifunctional signaling platform called ILK

(integrin linked kinase) through its interaction with a number of different signaling initiators (FAK, Src, ERK1/2, ILK, PI3K and JNK) (Legate et al. 2005). Hannigan et al. (1996) reported that ILK phosphorylated the cytoplasmic domain of β1 Integrin *in vitro*. Integrin activation has three temporal stages: 1) immediate effects (0-10 min) 2) short-term effects (10-60 min) 3) long-term effects (over 60 minutes). Integrin clustering activates lipid kinase, which upregulates phosphorylation of Src and FAK and increases concentration of phosphatidylinositol 4,5 bisphosphate (PIP2) and phosphatidylinositol 3,4,5 triphosphate (PIP3). These immediate effects are followed by the short-term effect, which concerns actin cytoskeleton organization. Long-term effects involve cell survival, proliferation and differentiation (Legate et al. 2009).

1.1.4 Macrophages Respond to Implants

Macrophages are the dominant cells that respond to various implant materials *in vivo* (Solheim et al. 2000) including metal (Takebe et al. 2003), ceramics and cements (Lu et al. 2002) and polymers (Solheim et al. 2000). Recognizing danger signals is the first step in macrophage response to foreign invasion (Xia & Triffitt 2006). Macrophages reaction to biomaterials is different from their respond to bacterial invasion as microbial infections are resolved by B and T lymphocytes activation, while biomaterial implantation results in inflammation and foreign body responses without B cells and T cells getting involved. Foreign body response includes foreign body giant cells, macrophages and fibroblasts and is dependent on the implant topography (James M Anderson 1988). Following the implant replacement, neutrophils migrate to the injury site to phagocytize microbes and later on macrophages arrive at the tissue–implant interface (James M. Anderson 1988; Martin & Leibovich 2005). Following the recognition of foreign materials, macrophages bind to the materials through adhesive interactions, which are mediated

by integrins (Anderson et al. 2008; García 2005). These interactions regulate macrophage function, including gene transcription, actin cytoskeleton rearrangement and cell proliferation (Berton & Lowell 1999).

It is thought that macrophages' interaction with implanted materials results in the activation and adhesion of cells as well as secretion of cytokines at the implant site (Anderson & Miller 1984). Macrophages exhibit rugophilia, that is they prefer rough surfaces over the smooth ones (Rich & Harris 1981) and significantly elongate on grooved substrata (Wojciak-Stothard et al. 1996).

1.1.5 Effects of Structured Surfaces on Cell Behavior

Takebe et al (2003) reported that expression of BMP-2 (an osteogenic growth factor) in J774A.1 macrophages increased on cpTi (commercially pure titanium) disks with surface roughness compared to smooth surfaces. Hamlet et al (2012) investigated the effect of surface roughness on genotypic cytokine expression in RAW264.7 macrophages cultured on polished and SLA surfaces for 24 hours. They reported that titanium surface topography was able to increase both pro and anti-inflammatory cytokines (IL-4, and IL-13) production. Ghrebi et al. (2012) studied the effects of polished, etched, blasted and SLA topographies on RAW264.7 macrophage morphology one day after culturing and they reported that macrophages were larger and more stretched on SLA surfaces compared to the polished, blasted and etched surfaces. Grooved surfaces can result in a phenomenon in macrophages called "contact or topographic guidance" which is the cell tendency to be oriented in its migration direction by the surface topography (Weiss 1945). Contact guidance has been studied using a variety of cell types and microfabricated substrata (Brunette 2001; Meyle et al. 1993; Curtis & Wilkinson 1998). Oakley and Brunette (1993) reported that microtubules are the first parts of the fibroblast cells

cytoskeleton that get aligned by the grooved topography. Surprisingly, they later found that fibroblasts lacking microtubules are still capable of getting aligned by the grooved topography, suggesting that although microtubules facilitate topographic guidance, they are not essential for this topographic regulation (Oakley & Brunette 1995). The size of surface features and their orientation affect the behavior of many cell types. Paul et al. (2008) reported that their microstructure surfaces produced by laser ablation were able to activate both M1 and M2 pathways in adherent macrophages while they could not find any significant effect of nanotextured surfaces on the macrophage chemokine secretion. Using human corneal epithelial cells, Teixeira et al. (2003) found that these cells were elongated and aligned along the both micro and nanoscale ridges. Zink et al. (2012) reported that combining nano and micro features can also influence cell behavior as the expression of osteopontin (a protein involved in bone remodeling) was increased in osteoblasts cultured on surfaces with combined features. It was also found that rough surface topographies can affect epithelial cells focal adhesion as more vinculin plaques were found localized at the ridges compared to the valleys (Baharloo et al. 2005). Chou et al. (1995) reported that grooved surfaces were able to elongate and align human gingival fibroblasts and increase mRNA level of fibronectin in these cells. It was also shown that surface chemistry and topography (V-shape grooved titanium) affect the cell morphology and gene expression and activity of metalloproteinase 2 (MMP-2) in human gingival fibroblasts (Chou et al. 1998). Fibroblasts were aligned along the grooves compared to the randomly oriented fibroblasts on smooth titanium (Ti). Also MMP-2 mRNA level was at significantly lower levels on Ti compared to the tissue culture plastic (Chou et al. 1998).

1.2 Overview of Implant Surface: Topography and Chemistry

Dental implant surface topography is an important factor in achieving osseointegration at the surgical interface (Cooper 2000) and numerous studies have reported that rough surface topographies enhance osseoconduction and osteogenesis (Cooper 2000; Chehroudi et al. 2009; Le Guéhennec et al. 2007; Cooper 2000). Sayles and Thomas (1978) state that topography can be defined as a narrow bandwidth of features that cover the form or shape of the surface. Surface topography can also be considered as the degree of roughness of the surface and the orientation of surface irregularities (Wennerberg et al. 2004). Surface topography can alter cell shape, which in turn alters cell functions (Hong & Brunette 1978) such as gene expression (Chou et al. 1998). Surface topographies can be smooth as polished surfaces (R_a value of 0.1 um or less) or have degrees of roughness as grit-blasted, acid-etched or sandblasted and acid-etched (SLA) surfaces. Topographic features can be in macro, micro or nano scales. SLA surfaces include both macro (sandblasted) and micro (acid-etched) features (Stanford 2008). Not only the surface topography but also surface chemistry affects protein adsorption to the implanted devices (Morra 2006). Surface chemistry modification may lead to the enhancement of tissue compatibility. Buser, Broggini, Wieland, et al. (2004) reported that their chemically enhanced SLA implant test surfaces exhibited a greater bone to implant contact at 2 and 4 weeks following the implantation. Their control surfaces were hydrophobic SLA implants while their modified surfaces were hydrophilic SLA implants with higher concentration of oxygen and titanium and lower carbon concentration compared to the test surfaces. Proteins, peptides and amino acids hold domains with different charges and therefore modifying surface charge (i.e. making implant surfaces positively or negatively charged) can facilitate protein absorbance to the implanted device (Textor et al. 2001). Although Brodbeck et al. (2002) could not find any significant differences

in the secretion levels of cytokines by monocytes and macrophages on the surfaces with different chemistry, they report a significant downregulation in the gene expression of IL-8 and upregulation in the gene expression of IL-10 in monocytes/ macrophages adherent to hydrophilic and anionic surfaces.

1.2.1 Surface Characterization

Surface characterization parameters can be divided into the profile (2D) values like R_a or the areal (3D) values like S_a. The R_a value is the most widely used parameter of roughness, which presents the arithmetic mean of the profile deviation from the mean line (Sittig et al. 1999). Wieland (1999) states that it is possible that two surfaces with the same R_a value act differently in a similar situation. Wennerberg and Albrektsson (2009) state that S_a value is a height-descriptive parameter like R_a, but it is used to measure the roughness over a surface in 3D dimensions. S_{al} and S_{tr} are two spatial parameters of 3D surfaces. S_{al} is defined as the fastest decay autocorrelation length (Reizer 2011; Dong et al. 1994) while S_{tr} is defined as the texture aspect ratio and is a parameter for identifying the texture pattern (Dong et al. 1994).

1.2.2 Surface Topography Fabrication

1.2.2.1 Isotropic Surfaces

Wennerberg and Albrektsson (2009) define isotropic surfaces as the surfaces with no oriented features, such as SLA (Sandblasted Large-grit Acid-etched) topography, which is produced by blasting Titanium with Al_2O_3 beads and acid etching by H_2SO_4 and HCl. SLA is a highly successful and widely used rough titanium implant surface that has been studied in detail (Buser et al. 2004; Perrin et al. 2002; Li et al. 2002).

1.2.2.2 Anisotropic Surfaces

According to Spencer and Moore (2001), anisotropic etching happens when etch rates perpendicular to the surface exceed etch rates parallel to the surface. Anisotropic etching is preferred when patterning surfaces. They also state that in the orientation-dependent anisotropic etching one face of the crystal is etched at a higher rate comparing to the others. Wennerberg and Albrektsson (2009) define anisotropic surfaces as the surfaces with clear orientations. The grooved surfaces as G1 and G2, studied in this thesis, are produced by anisotropic etching of Si <110> crystals. Silicon is widely used in micromachining as its different crystallographic directions have different etch rates. For example, the etch rate in the <110> or <100> directions are faster than the <111> direction (Brunette, Donald M., Tengvall, P., Textor, M., Thomsen 2001). Different chemicals can be used as the etchant for silicon but according to Sato et al. (1998) potassium hydroxide (KOH) is the preferred etchant.

Chapter 2: Statement of the Problem and Objectives

Problem: Although a number of investigators, including our research group, have studied effects of defined surface topographies on osseointegration and inflammatory responses (Waterfield et al. 2010; Ghrebi et al. 2013; Hamlet et al. 2012; Chehroudi et al. 2009; Cooper 1998; Refai et al. 2004; Puleo & Nanci 1999), it is not known which receptors and signaling pathways are involved in regulating these effects.

Hypothesis: We hypothesize that the galectin-3/ CD98/ integrin β1 cell-surface signaling complex is important for topography-directed linage determination.

Specific aims:

1. To study the effects of surface topography on RAW264.7 macrophages cytokine gene expression and cell morphology
2. To determine if galectin-3 plays a role in regulating topographical effects in RAW264.7 macrophages

Significance: Given the importance of macrophages in wound healing and osseointegration, it is important to understand the mechanisms whereby surface characteristics produce macrophage polarization in order to design a new generation of biomaterials that are capable of directing the innate immune system.

Chapter 3: Materials and Methods

3.1 Substrata and Preparation of Replica Surfaces

Four surface topographies were used in this study: Polished (PO), sandblasted and acid-etched (SLA) and two novel grooved surfaces, G1 and G2 (Figure 3-1), produced by anisotropic etching of Si <110> crystals (Figure 1). Commercially pure titanium (cpTi) disks of polished (PO) with R_a value of 0.06um (15mm in diameter and 1mm in thickness) and SLA with R_a value of 4.3um were kindly donated by Institute Straumann (Waldenburg, Switzerland). Grooved topographies designated as G1 and G2 were produced at the Advanced Materials and Process Engineering Laboratory (AMPEL) Advanced Nanofabrication Facility (ANF), UBC. G1 and G2 surface topography was measured at Department of Materials, Swiss Federal Institute of Technology Zurich (ETHZ) (Table 3-1). G1 surfaces with R_a value of 0.1um were fabricated by anisotropic etching technique using Si <110> crystals. Silicon wafers were first cleaned by the standard cleaning (SC) steps: SC1 and SC2. SC1 was performed with a solution of 5 parts of deionized water (DI), 1 part of aqueous NH_4OH (27% NH_3) and 1 part of aqueous H_2O_2 (30%) to remove organic residues. SC2 was performed with a solution of 6 parts of DI, 1 part of aqueous HCl (27%) and 30% of aqueous H_2O_2 (30%) to remove the metallic (ionic) contaminants. Following the standard cleaning, Si wafers went through a 30 seconds cleaning by 47% HF followed by a DI rinse. Then Si wafers (placed in a condenser top beaker assembly) were etched by freshly prepared KOH solution (75wt% of KOH, 23.5wt% of DI and 1.5wt% of isopropyl alcohol) at 70~90°C on a stirrer to obtain the desired surface topography. G2 surfaces with R_a value of 1.2um were produced by more vigorous anisotropic etching by raising the temperature up to 165°C. Characterization of G1 and G2 surfaces was performed using a Plu Neox (Sensofar, Spain) in the confocal mode. The analysis was conducted using Sensomap (v. 6.1, Sensofar,

Spain) and Matlab (v. R2014b, Mathworks, USA) for the isotropy parameters, setting the threshold of the autocorrelation function to 0.3. All the experiments in this study were performed on the epoxy replicates of these surfaces. Replicates were prepared with high precision according to previously published methods (Chehroudi 1988, Wieland 2002, Schuler 2009) and represented the original surface features with high fidelity. In brief impressions materials of the surfaces were made with Vinyl polysiloxane (Flexitime Light Flow; Heraeus Kulzer, Germany). These impressions were filled with epoxy resin (Epo-TEK 302-3M; Epoxy Technology, MA, USA) and cured overnight at 37°C (initial polymerization) followed by incubation for 6 hours at 58°C and 2 hours at 80°C. Epoxy replicas were cleaned by sonication in a 50% solution of the detergent 7X (MP Biomedicals, CA, USA) for 20 minutes followed by rinsing in distilled water and 10 minutes sonication in ultrapure water (NANO pure Diamond; Barnstead). Just before cell seeding the epoxy substrata were further cleaned and sterilized for 4 minutes in argon plasma (Plasma Cleaner/Sterilizer PDC-32G; Harrick Scientific).

Surface	Roughness Parameter	Isotropy Parameter
SLA	R_a (um) 5.50 +0.030	N/A N/A
G1	R_a (um) 0.10 $\pm$ 0.02	S_{tr} 0.03 $\pm$ 0.003 S_{al} (um) 2.10 $\pm$ 0.40
G2	R_a (um) 1.20 $\pm$ 0.25	S_{tr} 0.08 $\pm$ 0.011 S_{al} (um) 5.80 $\pm$ 1.50

Table 3-1 Topographic characteristics for SLA, G1 and G2 surfaces

Characterization of surface topography of SLA, G1 and G2 surfaces. Data present an average of 3 separate measurments $\pm$ standard deviation. The R_a value is the most widely used parameter of roughness, which presents the arithmetic mean of the profile deviation from the mean line. S_{al} (autocorrelation length) is a spatial parameter of a 3D surface and measures the distance over the surface such where the new location is statistically different from the original location. S_{tr} (texture aspect ratio) equals to the spatial isotropy or directionality of the surface texture. For highly anisotropic surface S_{tr} value is close to 0.00, while a spatially isotropic texture have a S_{tr} value closer to 1.00. G1 and G2 surface characterizations were done by Dr. CVM Cremmel (Swiss Federal Institute of Technology, Zurich). SLA characterization was done by Wieland (1999).

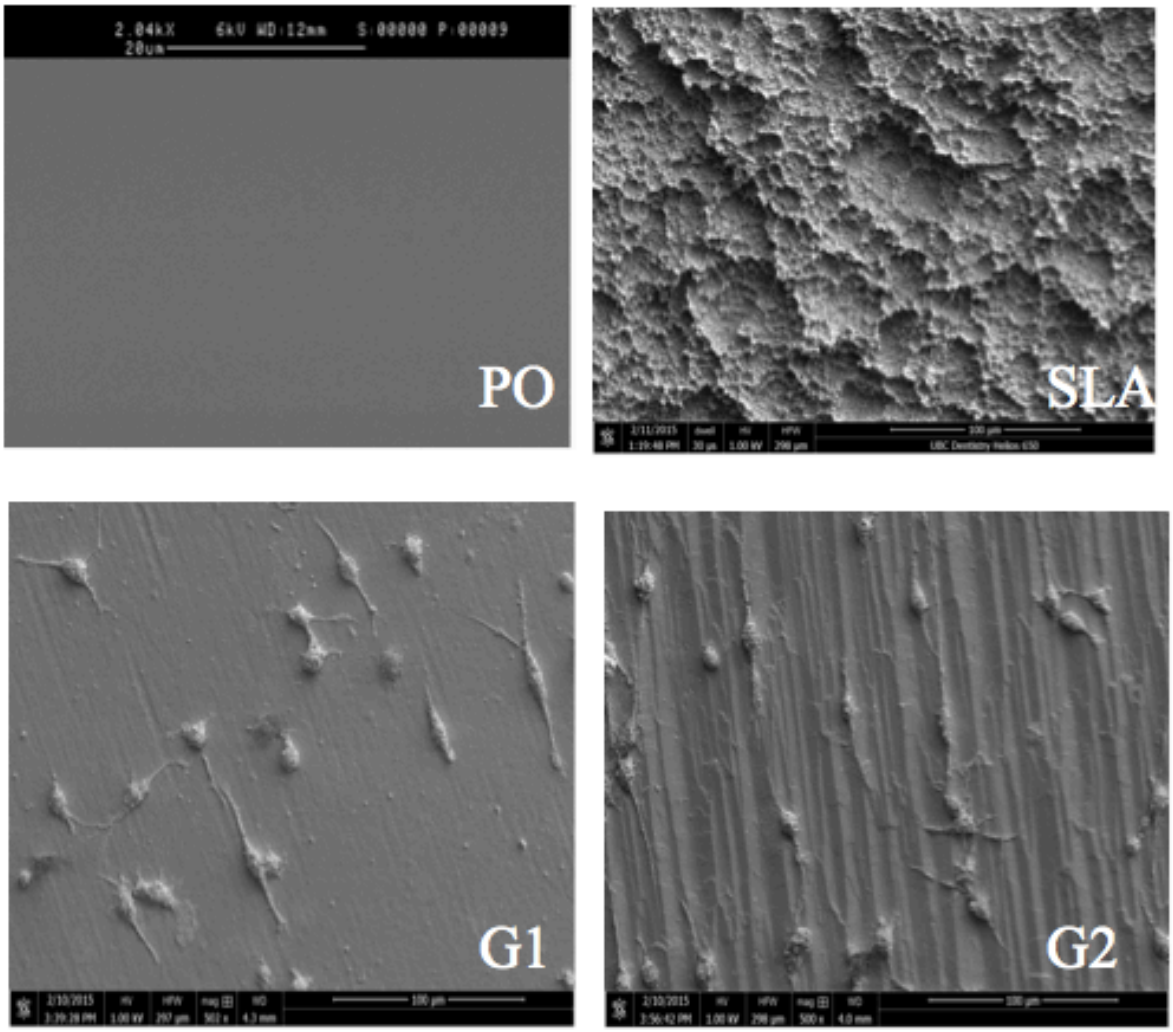

Figure 3-1 SEM micrographs of the epoxy replica samples: A) Polished (PO), B) SLA, C) G1 D) G2. Note that RAW264.7 cells are shown on the G1 and G2 surfaces.

3.2 Cell Culture and Inhibitors

For all the experiments in this study, murine macrophage-like cell line RAW264.7, obtained from American Type Culture Collection (ATCC, VA, USA) was used. RAW264.7 cells were cultured in 75cm^2 tissue culture flasks (Corning; VWR International, ON, Canada) in complete growth medium made of Dulbecco's Modified Eagle's Medium (Stemcell Technologies, Vancouver, Canada) supplemented with 10% heat-inactivated bovine growth serum (FGS) (Fisher Scientific, ON, Canada) and an antibiotic mixture containing 66ug/ml penicillin G (Sigma-Aldrich, Missouri, USA), 33ug/ml gentamycin sulfate (Gibco, NY, USA) and 0.7ug/ml amphotericin B (Gibco, NY, USA) at 37°C in a humidified atmosphere of 95% air and 5% CO2 (Barth et al., 2013). Cells used for experiments were passaged a maximum of 8 times after thawing as we noticed that macrophage response to topography was reduced when the passage number was higher than 7~8. Cells were plated onto the epoxy replicas at 2×10^5 cells/ml/well (Corning Costar, VWR International, ON, Canada) for all experiments. For a M2 phenotype control, macrophage cells were primed with 40 ng/ml IL-4 (Peprotech, Quebec, Canada) 30mins after seeding on PO substrata. Inhibitors were added to the media after 30 minutes following cell seeding to give the cells sufficient time to attach before treatment.

3.2.1 Lactose

D-Lactose monohydrate (50mM) (Sigma-Aldrich, Missouri, USA) was used as the inhibitor for galectin-3 function. Lactose blocks attachment of galectin-3 to its receptor CD98 on the macrophage's cell membrane (Hsu et al. 2000; Liu et al. 1995). D-Lactose stock solution was prepared by dissolving D-Lactose monohydrate (Sigma-Aldrich, Missouri, USA) in PBS. The

solution was gently heated to get a clear solution and then filtered by syringe filter 0.2 um (Fisher Scientific, MA, USA) before being added to the cell culture.

3.2.2 LY294002

PI3K inhibitor, LY294002 (10uM) (Sigma-Aldrich, Missouri, USA), (Fukao & Koyasu 2003; MacKinnon et al. 2008; Henderson et al. 2004), was dissolved in DMSO and was diluted with complete growth medium. The final concentration of DMSO (Sigma-Aldrich, Missouri, USA) in the cell medium was 0.05% (v/v) (0.5ul DMSO in 1000ul complete growth medium).

3.3 Cell Number (MTS Assay and DAPI Staining)

The number of viable cells on polished, SLA, G1, and G2 samples was quantified in the absence and presence of lactose, IL-4 and DMSO using DAPI staining method and the metabolic MTS assay. For DAPI staining cells were first washed twice (5 minutes each) with pre-warmed PBS. Then cells were fixed for 20 minutes at room temperature with 4% formaldehyde. They were then washed with PBS wash 3 times (5 minutes each). Next the cells were counterstained with DAPI prepared at 5ug/ml (Sigma Aldrich) for 30 minutes at room temperature. Samples were then washed 5 times (2 minutes each) and were mounted on slides. An Axio Scope 2 fluorescent microscope (Zeiss, Jena, Germany) was used for observing samples at 10x magnification. Cells were counted on each disc for 5 different areas (top, bottom, left, right and center of the disc) and pictures from each spot were taken by a RETIGA 1300 (QImaging, BC, Canada) connected to the microscope. ImageJ (image processing and analysis in Java) version 1.48r was used for counting number of cells per frame. The area of the field of view was 1.4 mm^2. Total average number of cells were calculated from two replicates per seeding.

The MTS assay was used to normalize the results from the protein secretion assay to the cell number on the respective substrata. Quantification was performed with the MTS containing CellTiter96® cell proliferation assay (Promega, WI, USA).

Supernatants were harvested for the cytokine and chemokine secretion assays. One ml of fresh cell culture medium and 200ul of the MTS reagent were added to a new 24 well plate (Falcon, NY, USA) and epoxy replicas were transferred to that well plate. After 2 hours incubation at 37°C in a humidified 5% CO_2 atmosphere, 130ul of the supernatants were transferred in triplicate to 96 well plates (Nalgen, NY, USA) and the absorbance of the formed formazan was measured at 490 nm on a microplate reader (FLUOstar Optima' BMG Labtech, Ortenberg, Germany). The absorbance of the sample was compared to a calibration curve that was obtained with each experiment and a known number of RAW264.7 macrophages up to $10x10^5$ cells.

3.4 SEM Observation of RAW264.7 Macrophages' Morphology

RAW264.7 cells plated on G1, G2, polished (PO) as well as Po+ IL4 (M2 phenotype control) for 24hrs were observed by scanning electron microscopy (SEM). Cells were first fixed with 2.5% glutaraldehyde (Fisher Scientific, ON, Canada) for 45mins. The samples were then rinsed with PBS. After PBS washing, cells were stained with 1% OsO_4 for 30mins then followed by 1% Tannic acid staining for 20mins. Lastly, samples were re-stained in 1% OsO_4 for 15mins. The subsequent dehydration steps were performed using a microwave (PELCO 3470 Hornet Microwave System, Pelco International, Redding, CA, USA). The specimens were then rinsed in 50, 60, 70, 80 and 90% ethanol 1min each and 2mins twice for 100% ethanol until finally 100% ethanol was exchanged with 100% hexamethyldisilazane (HMDS) (Sigma-Aldrich, MO, USA) for 3times 10mins each at room temperature. Then samples were sputter-coated with Iridium

using Leica EM MED020 Coating system (Leica, Wetzlar, Germany) and observed using Helios Nano Lab™ Dual Beam™ scanning electron microscope (FEI, OR, USA) at 1kV accelerating voltage at the UBC Centre for High-Throughput Phenogenomics.

3.5 Immunofluorescent Staining

To study the distribution of vinculin plaques and actin filaments, RAW264.7 macrophages were washed twice (5mins each) with pre-warmed PBS. Then cells were fixed by 4% formaldehyde (Fisher Scientific, MA, USA) + 0.1% Triton X-100 (Fisher Scientific, MA, USA) prepared in PBS for 10 minutes at room temperature followed by three washes (10 minutes each). Cells were blocked for 1 hour in 10% goat serum (Sigma-Aldrich) in 1% BSA in PBS at room temperature to reduce non-specific binding. Then samples were incubated with rabbit anti-mouse vinculin (1:100) (Santa Cruz Biotechnology, TX, USA) in 1% BSA in PBS at room temperature overnight at 4°C. Cells were washed six times with PBS (5minutes each) and subsequently samples were incubated with Alexa Fluor 488 goat anti-rabbit antibody (1:200) (Invitrogen, NY, USA) in 1% BSA in PBS at room temperature for 1 hour followed by two rinses with PBS. For actin staining, cells were stained with Phalloidin (1:500) (Sigma-Aldrich) in PBS for 40 minutes at room temperature followed by three PBS washes (1 minute each). To visualize cell nuclei samples were counterstained with DAPI prepared at 5ug/ml (Sigma-Aldrich) for 30 minutes at room temperature and were washed 5 times with PBS (2 minutes each). Finally samples were mounted on a slide in Fluoromount® (SouthernBiotech, AL, USA). Stained specimens were examined with a Nikon confocal microscope C1 and EZ-C1 3.50 software version 1.0. Confocal images were captured with a RETIGA 2000R camera (Q Imaging, BC, Canada). For each sample, field of view was selected as the left, right, top, bottom and the center of the disc and

settings were identical for all images. All confocal pictures were taken at 60x magnification and 3x digital zoom. Actin staining was used to detect the border of the cell for measuring the cell area with imageJ. For preparing 3D reconstructed images, Z-stacks of macrophages were captured at 0.5um intervals by Nikon confocal microscope and images were reconstructed into 3D format by imageJ.

3.6 RT-qPCR

Total RNA was isolated from $2x10^5$ macrophages with RNeasy Mini Kit (Qiagen,ON, Canada) according to the manufacturer's instructions (Qiagen, Germany). RNA quality and quantity was assessed with the Nanodrop ND-1000 Spectrophotometer (Thermo Fisher Scientific, MA, USA). RNA with 260/280 ratio >1.8 and 260/230 ratio >1.8 was considered pure and was used for making cDNA (Nolan, Hands & Bustin, 2006). cDNA was produced from total RNA (500ng) using an iScript cDNA synthesis Kit (Bio-Rad Labratories, CA, USA) and a Mastercycler gradient thermal cycler (Eppendorf, Hamburg, Germany) following the manufacturer's instructions. RT-qPCR was performed using a RG-3000 Rotor Gene PCR cycler (Corbett Research, NSW, Australia) and SsoFast™ EVA Green® Supermix Kit (Bio-Rad Laboratories, CA, USA). 40S ribosomal protein S18 (RPS18) was used as housekeeping gene to normalize cDNA samples. For each run of RT-qPCR a triplicate of NTC (no-template control) and nRTC (no-reverse-transcriptase control) were also included as negative controls. Relative quantification of transcript abundance was performed using the comparative $2^{-\Delta\Delta CT}$ method (Schmittgen & Livak 2008). Sequences for the primers used were as follows: mannose receptor (MR) forward primer: 5'-CAT GAG GCT TCT CCT GCT TCT-3', mannose receptor reverse primer: 5'-TTG CCG TCT GAA CTG AGA TGG-3', iNOS forward primer: 5'-CAG CTG GGC TGT ACA

AAC CTT-3', iNOS reverse primer: 5'-CAT TGG AAG TGA AGC GTT TCG-3', CCL2 (MCP1) forward primer: 5'AGG TGT CCC AAA GAA GCT GTA-3', CCL2 reverse primer: 5'-ATG TCT GGA CCC ATT CCT TCT-3', CCL3 (MIP1α) forward primer: 5'-TGA CAC TCT GCA ACC AAG TCT TC-3', CCL3 reverse primer: 5'-AAC GAT GAA TTG GCG TGG AA-3', CCL4 (MIP-1β) forward primer: 5'-TTC TCT TAC ACC TCC CGG CAG-3', CCL4 reverse primer: 5'-GTA CTC AGT GAC CCA GGG CTC A-3', CCL7 (MCP3) forward primer: 5'-AGC TAC AGA AGG ATC ACC AG-3', CCL7 reverse primer: 5'-CAC ATT CCT ACA GAC AGC TC-3', RPS18 forward primer: 5'-TCA TGC AGA ACC CAC GAC AGT ACA-3', RPS18 reverse primer: 5'-TGT TGT CTA GAC CGT TGG CCA GAA-3'. The Rotor Gene PCR cycler machine was set as follows: denaturing step for 1 minute at 95°C, then 40 cycles were performed for 10 seconds at 95°C and 60 seconds at 60°C.

3.7 Cytokine Microarray

To study the influence of surface roughness and lactose treatment on cytokine and chemokine secretion by RAW264.7 macrophages, a commercially available antibody array (Proteome Profiler, Mouse cytokine Array Panel A; R&D system, Minnesota, USA) was used according to the manufacturer's instructions. The array consists of 40 capture antibodies spotted in duplicate on a nitrocellulose membrane as following: BLC, C5a, G-CSF, GM-CSF, I-309, Eotaxin, sICAM-1, IFN-gamma, IL-1 alpha, IL-1 beta, IL-1ra, IL-2, IL-3, IL-4, IL-5, IL-6, IL-7, IL-10, IL-13, IL-12 p70, IL-16, IL-17, IL-23, IL-27, IP-10, I-TAC, KC, M-CSF, JE, MCP-1, MCP-5, MIG, MIP-1 alpha, MIp-1 beta, MIP-2, RANTES, SDF-1, TARC, TIMP-1, TNF-alpha, TREM-1. Microarray measurements are based on a sandwich ELISA principle. After blocking of the background, a mixture of detection antibody cocktail and supernatants was incubated overnight

at 4°C with the membranes. The amount of supernatant used was calculated according to the number of viable cells on the respective samples determined by the metabolic MTS assay (Promega, Wisconsin, USA). Captured proteins were labeled with a streptavidin functionalized IR-Dye (IRDye 800 CW streptavidin; LI-COR, NE, USA) and detected with a LI-COR Odyssey Infrared Imaging System. ImageJ (version 1.48r) was used to determine after background subtraction the integrated density of the spots on the array pictures.

3.8 Sandwich ELISA

Secretion level of MIP-1 alpha (CCL3) was measured in the presence and absence of lactose (50mM) on polished and grooved surfaces after day1 using sandwich ELISA following the manufacturer's instructions (Quantikin ELISA, Mouse CCL3/ MIP-1 alpha, R&D system). To determine the optical density of each well, a microplate reader (FLUOstar Optima; BMG Labtech, Ortenberg, Germany) was used which was set at 450 nm and corrected at 550 nm. A standard curve for determination of the amount of secreted chemokines was obtained by a four parameter logistic curve-fit with the BMG microplate reader software MARS (version 1.10). All samples were assayed in triplicate.

3.9 Statistical Analysis

For the cell area measurements and elongation factor, differences between different treatments were tested with One-Way ANOVA followed by a Tukey's post hoc test and p values <0.05 were considered significant. Results are shown as means $\pm$ SD. The RT-qPCR experiments were performed 2-8 times and the ratio Ct (Ct (treated)/ Ct (control)) was calculated. Results are

shown as means ± SD. Values were considered significant if the 95% confidence interval did not include the value of one.

Chapter 4: Results

4.1 Effects of Surface Topography and Lactose Treatment on RAW264.7 Macrophage Morphology

4.1.1 Scanning Electron Microscopy (SEM)

RAW264.7 macrophage cells were cultured on polished (PO), G1 and G2 surfaces for one day prior to processing SEM. As rough surfaces have a tendency to produce the alternatively-activated phenotype, we included IL-4-primed macrophages on PO surfaces as the positive control since it is known that IL-4 induces the M2 phenotype and also cell elongation (McWhorter et al. 2013). The effect of lactose treatment on macrophage morphology was determined by culturing cells on PO surfaces in the presence and absence of lactose (50mM) (Figure 4-1). Analysis of our SEM micrographs showed that lactose treated cells had significantly smaller area compared to the untreated cells and RAW264.7 cells were significantly more elongated when cultured on G1 surfaces compared to the PO surfaces or when treated with IL-4. Macrophages adherent to G2 surfaces were the most elongated among all groups (Figure 4-2).

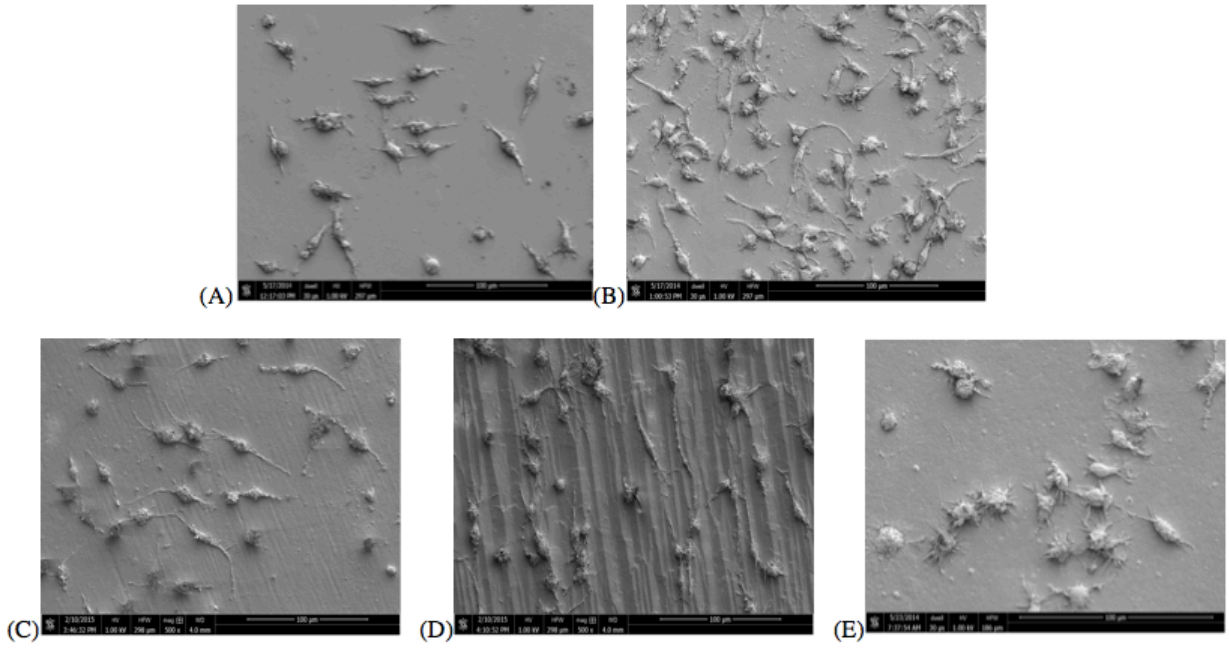

Figure 4-1 SEM micrographs of RAW264.7 macrophages. Cells were cultured on PO surfaces as the morphology control (A). Cells were cultured on PO surfaces in the presence of IL-4 as the positive control for alternatively activated morphology (B). Cells were cultured on G1 (C) and G2 (D) surfaces. (E) shows macrophages on PO surfaces in the presence of lactose (24hrs).

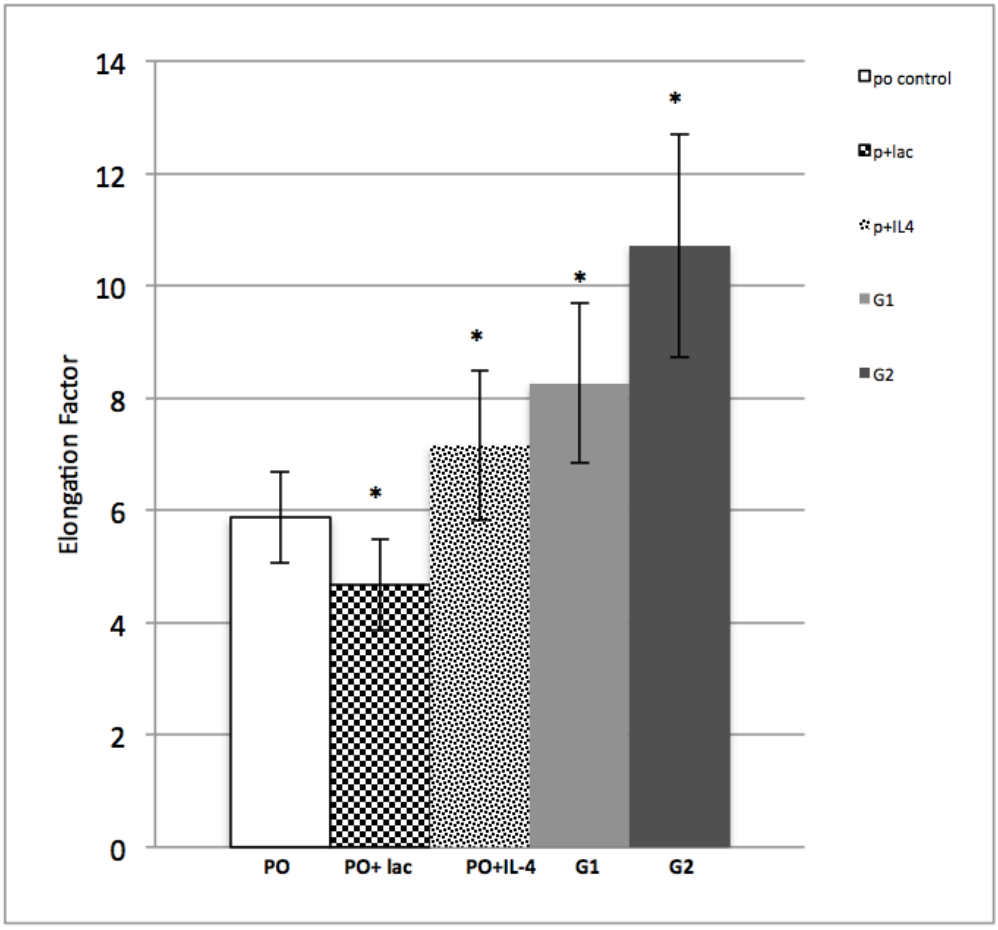

Figure 4-2 Quantification of cell elongation for macrophages on PO (control), PO+IL-4 (40ng/ml), G1, G2 and PO+lactose (50mM) surfaces after day1. Error bars indicate the SD for 30 cells measured per treatment. p <0.05 compared with control cells as determined by One-Way ANOVA followed by a Tukey's test. ImageJ software was used measuring the longest (major) axis and shortest (minor) axis of the cells. Elongation factor was defined as the ratio of the major to the minor (McWhorter et al. 2013). Means labeled with the asterisk are significantly different from the polished control group.

4.1.2 Immunofluorescent Staining and 3D Reconstruction of Confocal Images

Macrophage cells were cultured on PO, G1 and G2 surfaces for one day and fluorescent staining and confocal microscopy used to study the effect of surface topography on macrophage morphology. As figure 4-3 demonstrates, 3D reconstructed confocal images of RAW264.7 exhibited a more spread morphology on G2 surfaces compared to PO and G1 surfaces after one day. The same pattern was observed in repeated experiments: A smaller area on PO and G1 surfaces compared to G2 surfaces (Figure 4-4). In the presence of lactose cells exhibited a reduced area on all topographies compared to untreated cells (Figure 4-5). We were not able to discern any differences in the distribution of actin filaments and vinculin plaques among the different topographies in the presence or absence of lactose.

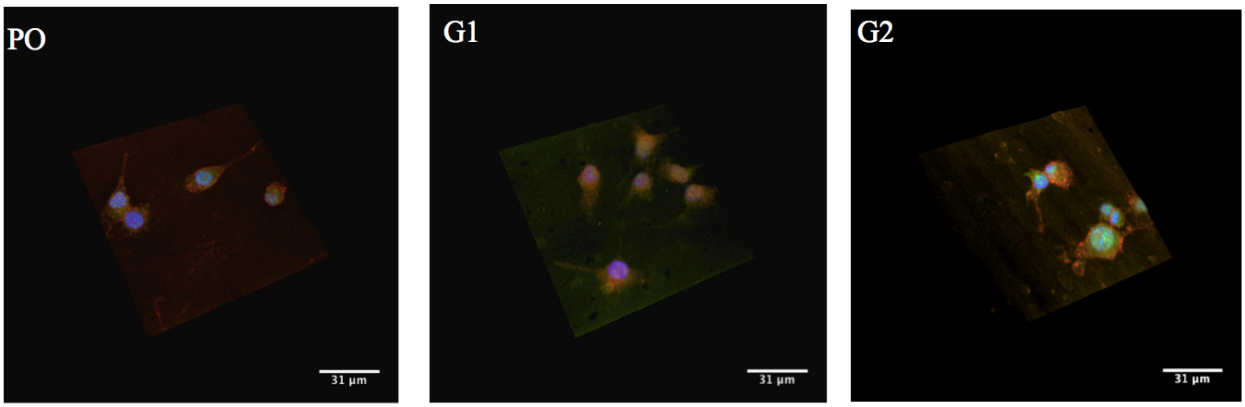

Figure 4-3 Reconstructed 3D images of fluorescent staining of macrophage cells at the one day of culture. Nuclei, blue; vinculin plaques, green; actin filaments, red. Cells are well spread on G2 surfaces comparing to PO and G1 samples. Z-stacks of confocal images were reconstructed into 3D images using imageJ. All images were taken at 60x magnification and a 3x digital zoom. All 3D images are presented at the same angle.

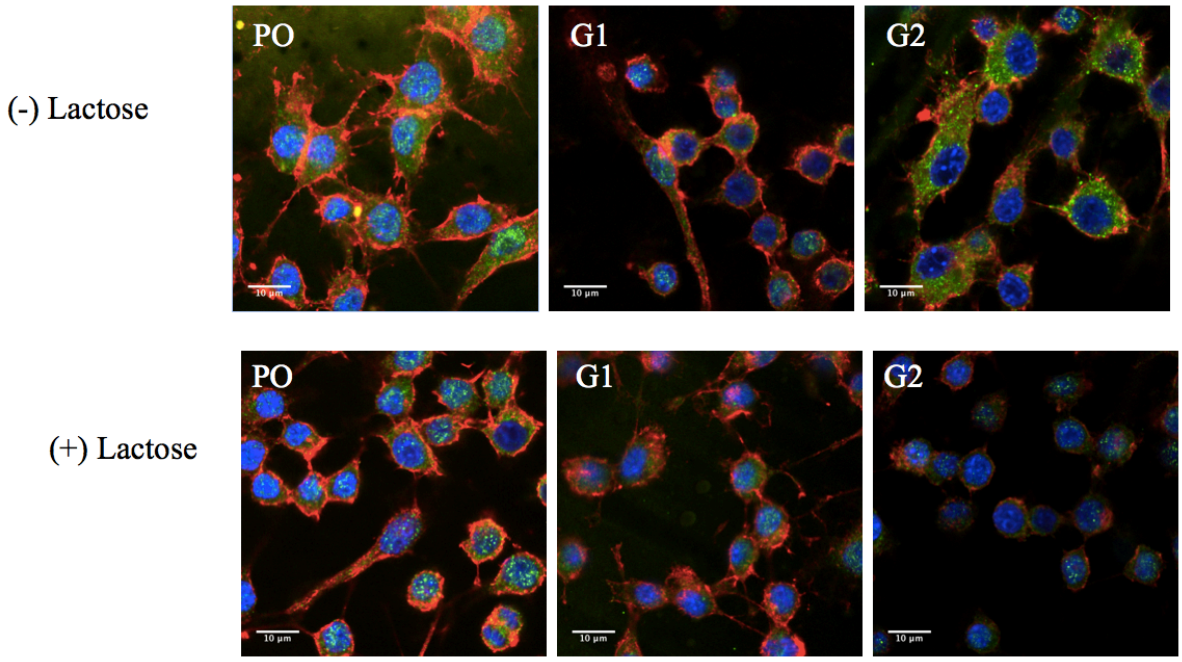

Figure 4-4 RAW 264.7 cells cultured on PO, G1 and G2 surfaces in the presence and absence of lactose (50mM) (Day1). Nuclei: blue; vinculin plaques: green; actin filaments: red. In the absence of lactose cells on G2 surfaces look more spread compared to PO and G1 surfaces. In the presence of lactose, cells look rounded up on all topographies. We could not discern any meaningful difference between vinculin plaques (size/shape) on different topographies in the presence and absence of lactose. All images are taken at 60x magnification and a 3x digital zoom.

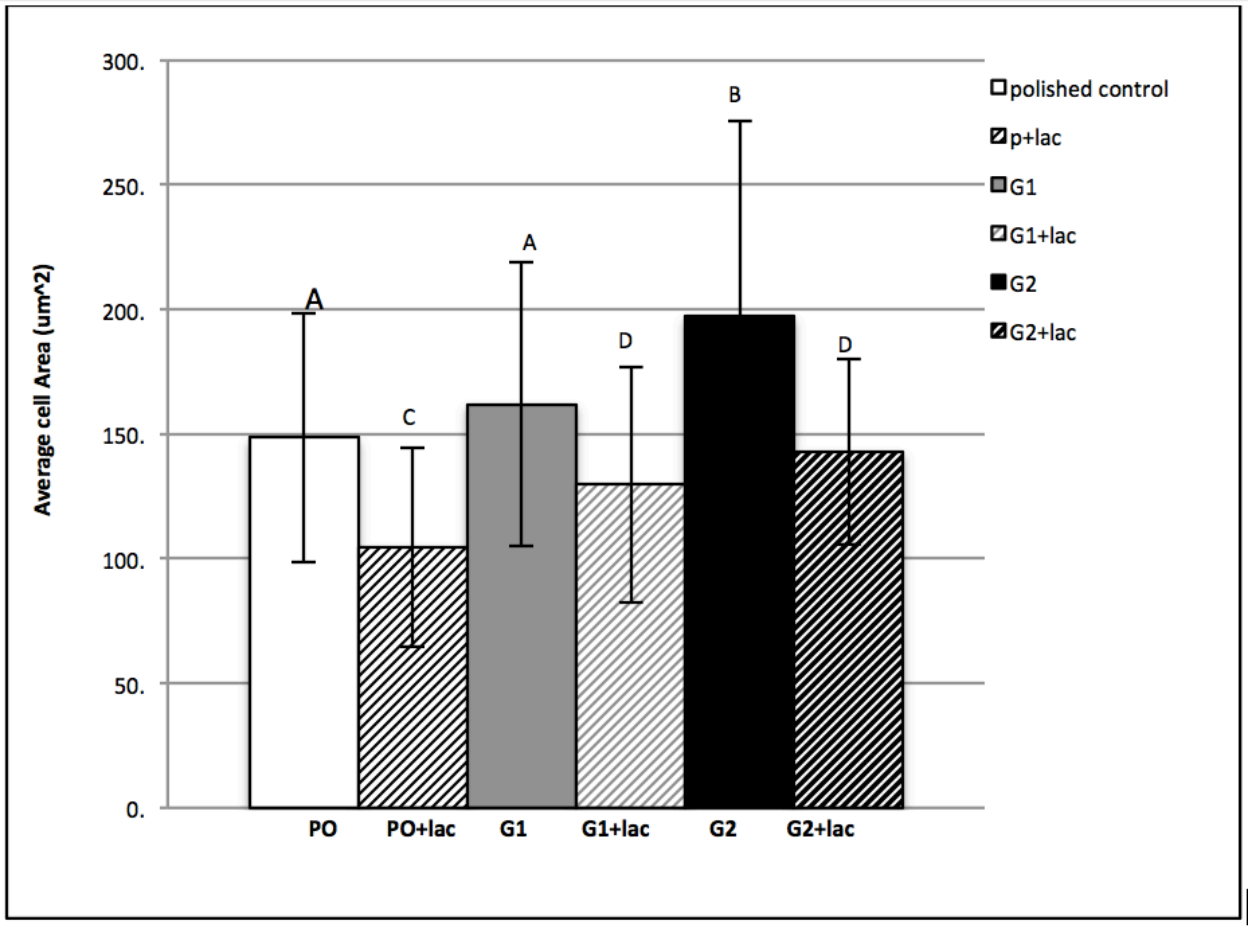

Figure 4-5 Quantification of cell area of macrophages cultured on PO (control), G1 and G2 surfaces in the presence and absence of lactose. Error bars indicate the SD for 30 cells measured per treatment. The area of each cell was determined by tracing the cell outline and was measured by ImageJ. Means labeled with different letters are significantly different. For example PO and G1 are not significantly different from each other while G2 is significantly higher than both PO and G1. Data were analyzed using One-Way ANOVA followed by a Tukey's post hoc test. $p < 0.05$.

4.2 RAW264.7 Macrophages Response to IL-4

To test the ability of RAW264.7 cells to respond to a known inducer of the M2 phenotype, we measured the gene expression of an M2 (MR) and an M1 (iNOS) marker in response to IL-4 (40ng/ml) on PO surfaces (Fig 4-6). As expected, MR gene expression was significantly upregulated in primed macrophages while iNOS gene expression was significantly downregulated in the presence of IL-4 after 24 hours of incubation.

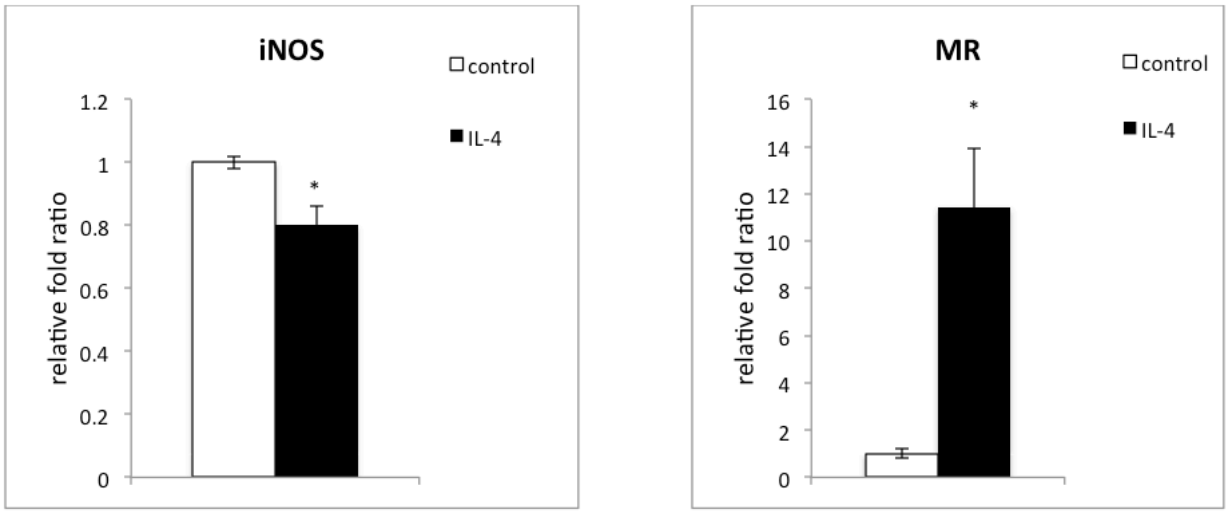

Figure 4-6 The average expression level of mannose receptor (MR) and iNOS in primed RAW264.7 macrophages with IL-4 (40ng/ml) on PO epoxy substrata after 1 day as measured by RT-qPCR. Target genes mRNA levels were normalized to RPS18 mRNA and represented as a relative fold ratio to the gene expression on PO surfaces. Values show mean $\pm$ SD (n=2). Statistically significant if the 95% confidence interval calculated for averaged ratio did not include the value of one (*).

4.3 Effect of Surface Topography and Lactose Treatment on RAW264.7 Macrophage Gene Expression by RT-qPCR

To further characterize the effect of smooth and rough topographies on macrophage phenotype, we measured gene expression of mannose receptor (M2 marker) and iNOS (M1 marker) as well as a group of chemokines including: MCP1/CCL2, CCL3/MIP1α, CCL4/MIP1β and CCL7/MCP3 on PO, SLA, G1 and G2 surfaces after one day of culture. The SLA surface has been widely and successfully used in dental implantology and has been shown to influence the inflammatory response of macrophages (Refai et al. 2004; Waterfield et al. 2010; Tan et al. 2006). As figure 4-7 illustrates, mannose receptor and iNOS expression were altered by rough topography as MR expression was significantly upregulated on G1 surfaces and iNOS was significantly downregulated on G2 surfaces relative to PO controls after day one. Gene expression of all chemokines was up regulated on G2 surfaces compared to the polished surfaces. CCL2, CCL3 and CCL4 were significantly upregulated on G1 surfaces.

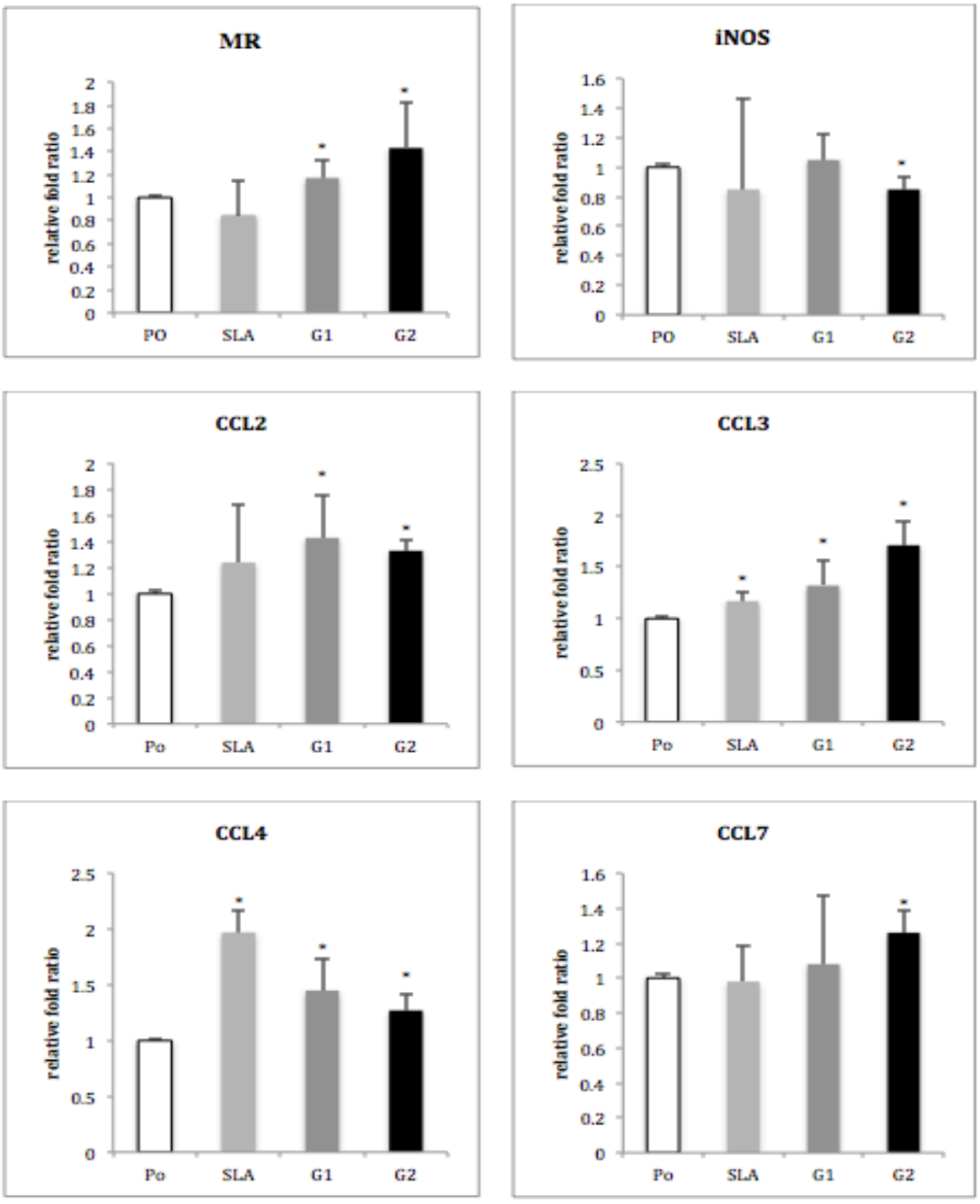

Figure 4-7 The average expression level of MR, iNOS, CCL2/MCP1, CCL3/MIP1α, CCL4/MIP1β and CCL7/MCP3 in RAW264.7 macrophages on PO, SLA, G1 and G2 substrata after 1 day as measured by RT-qPCR. Target genes mRNA levels were normalized to RPS18 mRNA and represented as a relative fold ratio to the gene expression on PO surfaces. Values show mean ± SD

of 2-8 separate experiments. Statistically significant if the 95% confidence interval calculated for averaged ratio did not include the value of one (*).

As figure 4-8 shows, adding lactose to the media, downregulated gene expression of mannose receptor by almost 50% on PO, SLA and G1 topographies compared to the control samples. Gene expression of iNOS was mostly upregulated on SLA surfaces (2 fold) followed by a significant upregulation on G1 (~1.9 fold) and PO (~1.4 fold) surfaces. CCL2/MCP1 gene expression was significantly downregulated on all topographies, while CCL3, which is a macrophage inflammatory protein, was significantly upregulated on both smooth and rough topographies in the presence of lactose. CCL4/MIP1β and CCL7/MCP3 expressions were not significantly affected by lactose treatment on either smooth or rough topographies (Fig 4-8).

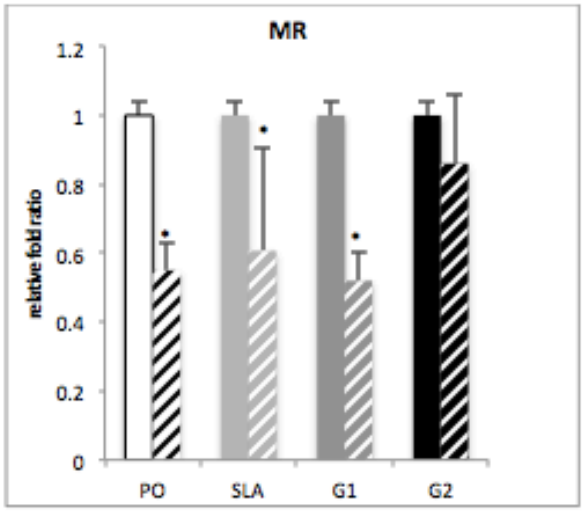
MR
relative fold ratio
1.2
1
0.8
0.6
0.4
0.2
0
PO
SLA
G1
G2

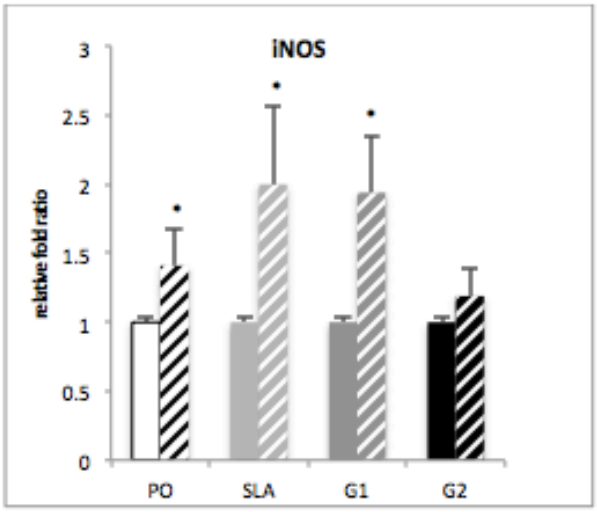
iNOS
relative fold ratio
3
2.5
2
1.5
1
0.5
0
PO
SLA
G1
G2

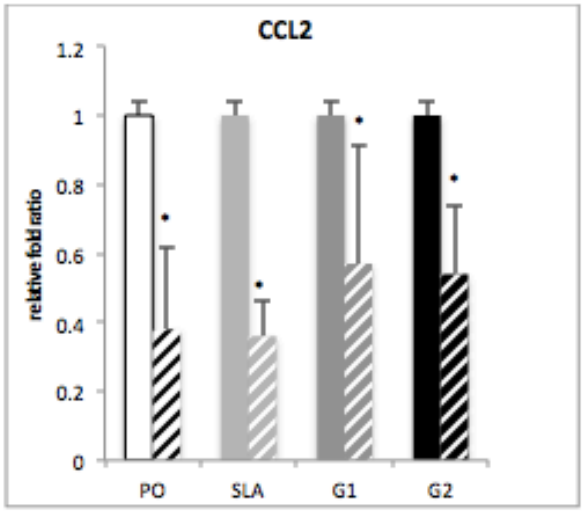
CCL2
relative fold ratio
1.2
1
0.8
0.6
0.4
0.2
0
PO
SLA
G1
G2

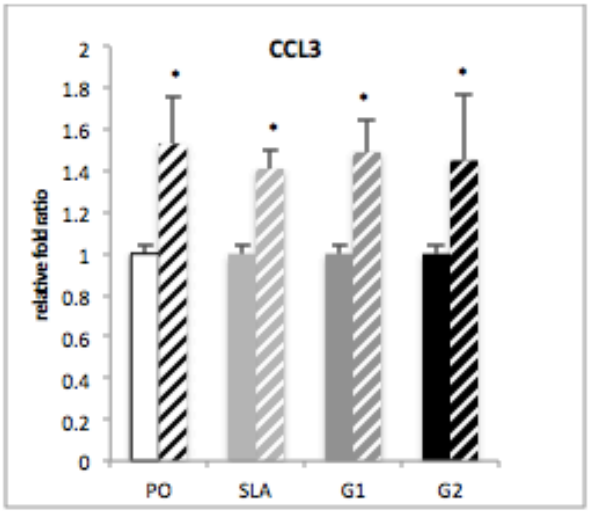
CCL3
relative fold ratio
2
1.8
1.6
1.4
1.2
1
0.8
0.6
0.4
0.2
0
PO
SLA
G1
G2

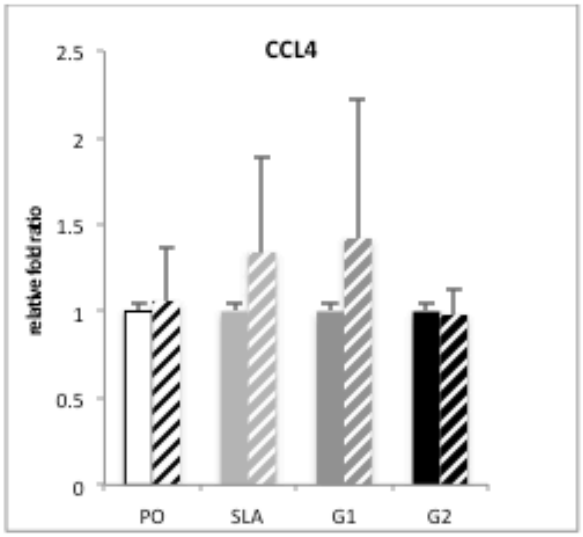
CCL4
relative fold ratio
2.5
2
1.5
1
0.5
0
PO
SLA
G1
G2

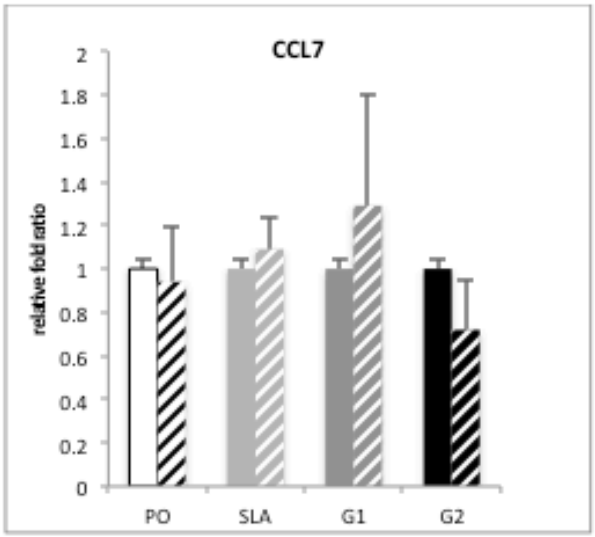
CCL7
relative fold ratio
2
1.8
1.6
1.4
1.2
1
0.8
0.6
0.4
0.2
0
PO
SLA
G1
G2

Figure 4-8 Effect of lactose treatment on the gene expression of MR, iNOS, CCL2/MCP1, CCL3/MIP1α, CCL4/MIP1β and CCL7/MCP3 in RAW264.7 macrophages on PO, SLA, G1 and G2 substrata after 1 day as measured by RT-qPCR. Target genes mRNA levels were normalized to RPS18 mRNA and represented as a relative fold ratio to the gene expression on each topography. Values show mean ± SD of 2-8 separate experiments. Statistically significant if the 95% confidence interval calculated for averaged ratio did not include the value of one (*). Bars with the striped pattern represent the gene expression in the presence of lactose (50mM).

4.4 Inhibition of PI3K Activity in RAW264.7 Cells by LY294002

PI3K is an important mediator of regulation of gene expression by IL-4 and priming macrophages by IL-4 results in alternative activation (Nelms et al. 1999). To investigate the role of PI3K in regulating topographical effects in RAW264.7 macrophage cells we blocked PI3K with LY294002 (10uM) and observed the effect on activation of RAW264.7 cells cultured on smooth and rough topographies. In these experiments, cells were not primed by IL-4, and the G1 surface itself was used to induce a M2-like phenotype. RT-qPCR was used to measure the gene expression of mannose receptor (M2 marker) in macrophages cultured on PO and G1 surfaces after 24hours of incubation in the presence and absence of LY294002 (Fig 4-9). Expression of mannose receptor was significantly downregulated on both PO and G1 topography in the presence of LY294002.

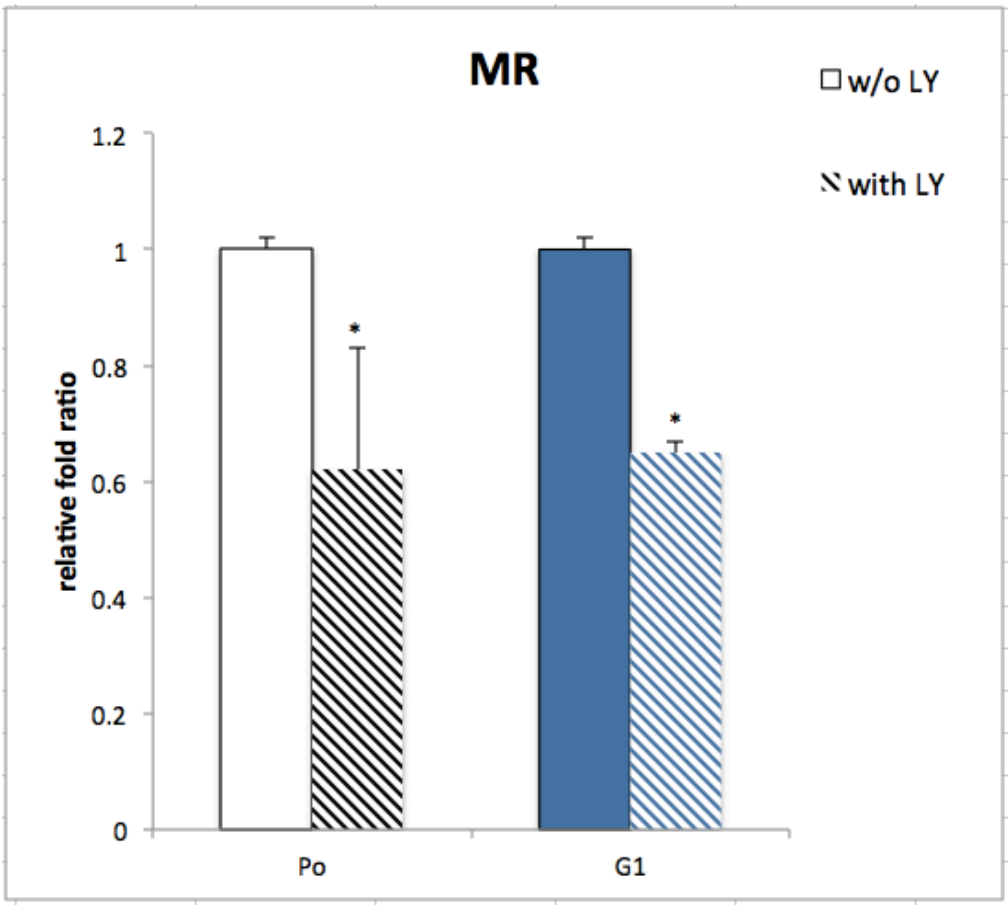

Figure 4-9 The average expression level of MR in RAW264.7 macrophages on PO and G1 substrata in the presence of LY294002 after 1 day as measured by RT-qPCR. Target genes mRNA levels were normalized to RPS18 mRNA and represented as a relative fold ratio to the gene expression on each topography. Values show mean ± SD (n=2). Statistically significant if the 95% confidence interval calculated for averaged ratio did not include the value of one (*).

Chapter 5: Discussion, Conclusions and Future Directions

5.1 Discussion

Implanted biomaterials have been shown to activate various components of the non-specific immune response known collectively as the "foreign body" response. Macrophages are an important member of this foreign body response and can be found at the site of biomaterial implantation (Chehroudi et al. 2009). As macrophages are "plastic cells" involved in both the inflammatory immune response and tissue remodeling it is important to determine whether biomaterials can modulate macrophage function. This question was addressed using four well-defined surface topographies to assess the topographical effect on polarizing RAW264.7 macrophages to an M1 or M2 phenotype as assessed by gene expression and cell morphology.

It was also hypothesized that topographic control of phenotype selection would be mediated by integrins as these extra-cellular matrix binding membrane receptors are in intimate contact with the topography through recognition of adsorbed serum proteins. Our study was based on the findings of MacKinnon et al. (2008) and Henderson et al. (2004), who demonstrated that galectin-3, CD98 and integrin were required for IL-4 induced alternate activation of macrophages. Galectin-3 is known to bind to CD98. Physical association of this complex with β1 containing integrin molecules increases their binding affinity to their respective ligands. Consequently in our study the role of the galectin-3/ CD98/ integrin β1 complex on selection of macrophage phenotype was evaluated. To test our hypothesis, galectin-3 attachment to its receptor CD98 was inhibited by lactose and the effects of lactose treatment on cell morphology, the expression of M1 and M2 markers and cytokines were measured.

5.2 Effects of Surface Topography and Lactose Treatment on RAW264.7 Macrophage Morphology

Observations of the effect of topography and lactose inhibition on cell morphology support the role of PI3K on cell shape and phenotype selection. Analysis of cell shape using confocal microscopy images, show that macrophages were more spread on rough topographies after day one compared to cells on smooth control surfaces. These observations agree with Wojciak-Stothard et al. (1996) who reported that at early times, macrophages were round on smooth surfaces and more spread on grooved surfaces. As PI3K has been shown to be important in integrin β1-mediated cell spreading in various cell types (Chun 2003) it is likely that PI3K is more activated on rough grooved topographies stimulating an elongated morphology characteristic of M2-polarized cells. Vinculin plaques were detected on both smooth and grooved surfaces at the focal contacts, using confocal microscopy. However, it was not possible to quantify differences in distribution and size of the vinculin plaques on the test surfaces. It is possible that a higher resolution technique such as SEM may reveal differences. For example Baharloo et al. (2005) reported vinculin plaques localization in epithelial cells at the ridges of the rough topographies using immunogold staining with SEM. Also, Ghrebi et al. (2013) studied effects of different surface topographies (etched, blasted and SLA) on RAW264.7 macrophage cell shape and reported that surface topography modulated cell shape and spreading and these changes were associated with changes in the distribution of vinculin.

Analysis of the cell shape of the RAW264.7 macrophages cultured on PO control surfaces in the presence and absence of IL-4 and also G1 and G2 surfaces by SEM showed that compared to the PO control samples macrophages were significantly more elongated on G1 and G2 surfaces. This elongation was similar to that seen with IL-4-stimulated cells. Macrophage elongation on

grooved surfaces can suggest that these surfaces modulated the cell phenotype toward M2 supporting the observation of McWhorter et al. (2013) who reported that macrophage cell elongation triggers an M2 polarization.

Lactose reduced cell area on all topographies. This smaller cells area is most likely a consequence of lactose inhibition of CD98 complex activated PI3K. As PI3K regulates actin assembly and cytoskeletal organization (Jiménez et al. 2000) its downregulation would be expected to affect the actin polymerization as well as diminish cell spreading and thus inhibit the formation of an M2-like morphology. The resultant round morphology is associated with activation of M1 phenotype (Edin et al. 2013; McWhorter 2013).

5.3 Effect of Surface Topography and Lactose Treatment on RAW264.7 Macrophage Gene Expression by RT-qPCR

On rough surface topographies such as the G1 and G2 surfaces in these experiments or the SLA surfaces studied previously in our lab (Barth et al. 2013) the phenotype relative to smooth surfaces is skewed towards the M2 phenotype. This phenotype shift was seen both in the gene expression profiles of cytokines and other markers of phenotype and in the development of an elongated cell morphology similar to that of IL-4-induced M2 macrophages. Cell alignment and elongation on grooved surfaces have been reported in many studies in a variety of cell types (reviewed by Brunette, 2001).

More specific information relevant to the signaling pathways and receptors that regulate the M1 and M2 phenotype can be obtained from gene expression studies of M1 and M2 markers and profiles of the chemokine expression. When different surface topographies (polished, blasted, acid-etched and SLA) were tested for M1 cytokine and chemokine production by Refai et al.

(2004) they reported that responses were very weak without the added stimulus of suboptimal concentrations of the M1 generating stimulator LPS. They did report a non-LPS driven effect in that CCL2/MCP1 and CCL4/MIP1alpha were significantly lower in SLA stimulated macrophages over a five day period. They concluded that surface topography can contribute to low levels of inflammatory signaling. Induction of a robust inflammatory response to titanium implants/ and their surface topography, however, is not possible unless a second signal (LPS) is present. Results reported in this thesis, support previous findings in our lab (Waterfield et al. 2010; Refai et al. 2004) in that rough surfaces moderately alter the gene expression of chemoattractants. The mannose receptor (M2 marker) is upregulated on G1 surfaces while iNOS (M1 marker) is slightly downregulated on G2 topography thus suggest that the grooved surfaces are capable of skewing macrophages toward alternative (M2) phenotype. Our findings are in agreement with of Martinez and Gordon assertion (2014) that adhesion molecules, extracellular matrix and chemokines contribute to the stimuli involved in macrophage polarization. Using different surface topographies as stimuli in which integrins in focal adhesions/ podosomes are in intimate contact with the topographies we propose that these membrane components can be added to the list of lineage-determining cell surface receptors.

Although statistically significant differences in gene expression occurred, the size of the effects were modest compared to the effect size seen when known modulators of macrophage phenotype such as IL-4 (for M2 induction) and LPS (for M1 production) were used. This modest shift towards a wound healing phenotype could nonetheless have significant effects when rough surfaces are implanted *in vivo*, as the rough surface would be an abiding influence that could recruit and polarize macrophages during the lifetime of the implanted device.

In the current experiments, the low affinity competitive inhibitor, lactose, presumably interfered with the attachment of galectin-3 to its receptor CD98 and consequently reduced the formation of galectin-3/ CD98/ integrin β1 signaling complex. This, in turn would be expected to downregulate PI3K signaling (MacKinnon et al. 2008) and it is known that downregulating PI3K signaling enhances inflammatory responses (Fukao & Koyasu 2003; Martinez 2011). In confirmation of that expectation, an increase in the M1 phenotype marker iNOS was observed in lactose-treated cells.

Lactose treatment also altered the chemokine secretion profile in macrophages as it downregulated CCL2 and upregulated CCL3 expression on all topographies but had no significant effect on CCL4/ MIP1α and CCL7/ MCP3 expression. CCL2 has been implicated in promoting an M2 phenotype as it has a beneficial effect in wound repair and its absence results in delayed wound healing (Dipietro et al. 1998). Although Gordon (2003) suggested CCL2 as an M2 marker, Mantovani et al. (2004) stated that CCL2 can be stimulated by the inflammatory phenotype stimulator LPS as well as the M2 phenotype inducer IL-4/IL-13. In any case the downregulation of CCL2 is at least consistent with the macrophages adopting a less M2-shifted phenotype in the presence of lactose.

5.4 Inhibiting PI3K Activity in RAW264.7 Cells by LY294002

In addition, as galectin-3/ CD98/ integrin β1 complex has been linked to PI3K activation we tested the effect of PI3K specific inhibitor, LY294002, on macrophage gene expression. We found that LY294002 downregulates the M2 marker on both rough and smooth topographies. These findings agree with MacKinnon et al. (2008) who reported that PI3K activation plays a key role in activating alternative phenotype in macrophages. It thus appears that in the absence of exogenously added cytokines or inflammatory stimuli the galectin-3/ CD98/ integrin complex

regulates the balance of M1 and M2 expression through PI3K and its associated pathways on both grooved and smooth surfaces.

5.5 The Hypothetical Model of Macrophage Polarization in The Presence and Absence of Lactose

The results reported in this thesis as well as previous results from our laboratory, including the work of Waterfield et al. (2010) suggest a model for galectin-3 in directing polarization of macrophages on smooth and rough topographies in the presence and absence of lactose (Figure 5-1). Waterfield et al. (2010) investigated early NFkB signaling and suggested that the signal transducer enzymes PI3K and AKT were involved in macrophage response to different topographies. NFkB isoforms rapidly activates a number of transcription factors having a multitude of inflammatory and anti-inflammatory functions. They also reported a role for lipid rafts in surface topography dependent activation of the proinflammatory cytokine IL-1β through the NFkB pathway. Membrane lipid rafts have been shown to orchestrate the assembly of cell-surface signaling proteins at the plasma membrane. Surface topography affects the spatial control of raft organization of lipids and signaling complexes. For example on SLA surfaces the lipid rafts become more susceptible to the effects of methyl- β-cyclodextrin on cholesterol-enriched-raft-associated signaling structures (Waterfield et al. 2010). Taken together with our previous findings on IL-1β we propose that localization of β1 integrin signaling complexes in lipid rafts plays a key role in regulating integrin activation. The effects of the different surface topographies noted may reflect changes in spatial control over the clustering of the above-mentioned raft associated signaling platform. This in turn would allow more efficient interactions with membrane associated signaling molecules and activation of downstream

signaling pathways. It could also promote actin assembly by concentrating molecules involved in actin polymerization thereby affecting cellular morphology/ polarity.

As figure 5-1 illustrates, galectin-3 binds to its receptor CD98 on the macrophage membrane and the combination of gal-3 and CD98 enhances association with integrin β1. Complex of galectin-3/ CD98/ integrin β1 regulates PI3K activation. PI3K has been linked to activation of the M2 phenotype by a decrease in the Src homology 2-domain-containing inositol-5′-phosphatase (SHIP) protein. Macrophages from SHIP-deficient mice have been shown to have an increased level of alternative activation markers. Decreasing levels of SHIP have been linked to both the PI3K pathway and STAT6 activity suggesting that these pathways are both important regulators of M2 function (Weisser et al. 1998; Zhou et al. 2014).

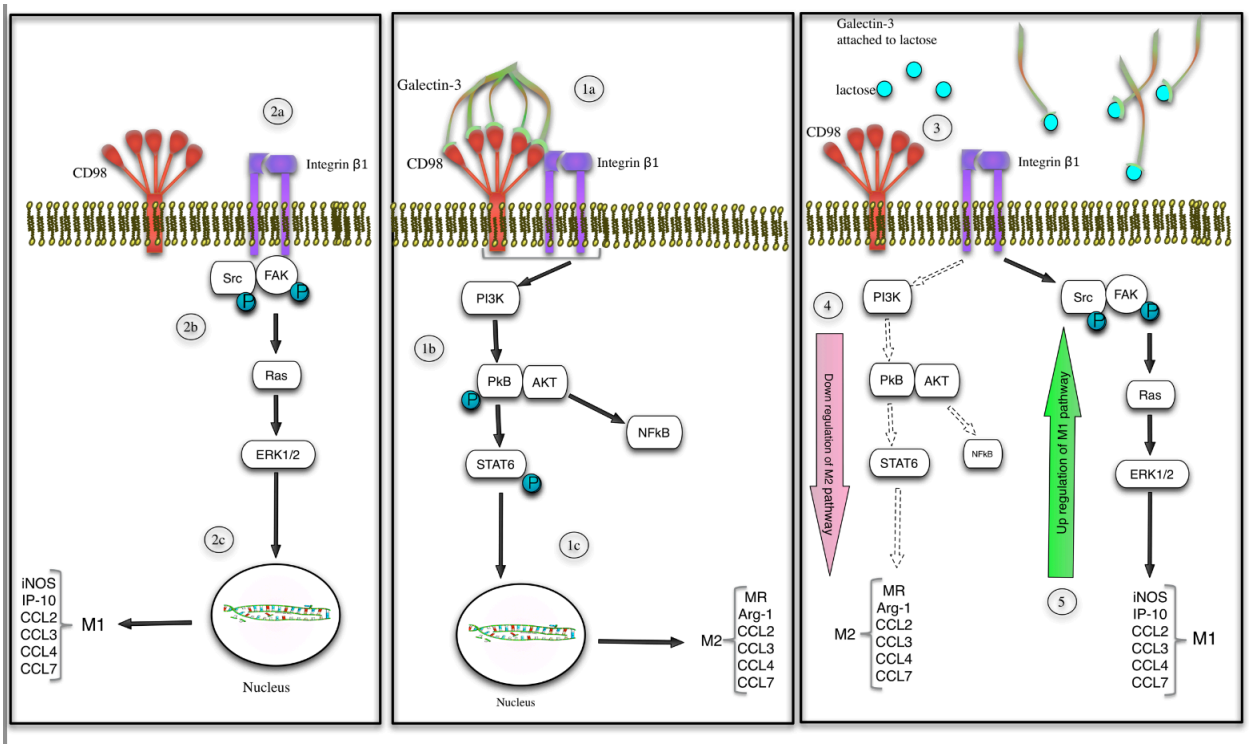

Figure 5-1 Hypothetical model of M1 and M2 pathways activation in macrophages in the presence and absence of lactose. Upon ligation of the integrin molecule available galectin-3 binds to its receptor CD98 allowing CD98 to interact with integrin (1a). Complexes of Gal-3/CD98/integrin activate PI3K resulting in downstream phosphorylation and nuclear translocation of the Stat-6-dependent M2 pathway (1b) and expression of M2 markers (1c). The M1 pathway is Gal-3/CD98 independent (2a). Ligation of the integrin molecule activates the M1 pathway and expression of M1 markers by phosphorylation of FAK/Src (2b) and the downstream phosphorylation and translocation of ERK ½ translocation factor activators (2c). In the presence of lactose, galectin-3 binds to lactose and is not able to bind to CD98 (3). Consequently, M2 pathway gets downregulated (4) and M1 pathway gets upregulated (5).

In the presence of lactose, attachment of gal-3 to CD98 is blocked and therefore the complex of galectin-3/ CD98/ integrin β1 cannot form. Consequently, the PI3K pathway is downregulated, resulting in upregulation of phosphorylation of focal adhesion kinase (FAK) and Src and activation of ERK1/2 pathway and production of M1 markers like iNOS and other chemokines. This is supported by an earlier study from our laboratory by Ghrebi et al. (2013) who tested the effect of surface topography on activation of the ERK1/2 inflammatory signaling pathway. We reported a topographical activation of FAK, Src and ERK1/2 in a time dependent manner. They also noted that macrophages on SLA at day three appeared to be downregulating the proinflammatory pathway more than the other surfaces tested.

Martinez and Gordon (2014) have summarized the data on macrophage polarization and concluded that the wide variety of external stimuli targeting macrophages through a number of different recognition receptors probably generate a mixed phenotype of cells in any given tissue. They propose a new multipolar view of the factors affecting macrophage activation where more than one stimulus has to be taken into consideration when macrophage polarization is considered as would be expected to be found in tissues in infected or diseased states. The findings we report in this thesis are in agreement with their view that adhesion molecules, extracellular matrix and chemokines contribute to the stimuli involved in macrophage polarization.

5.6 How Might Galectin-3 Regulate The Effects of Surface Topography on Macrophages?

At a molecular level we can only speculate how galectin-3 can mediate this effect. It is clear that there is more than one integrin dimer combination capable of recognition of fibronectin adherent to the different surface topographies. Each is capable of recruiting different adaptor molecules to

the cytoplasmic membrane that are responsible for the initiating a wide variety of macrophage responses. It is possible that galectin-3/ CD98 complex selects specific dimer combination(s) that result in cell polarization/ morphological changes. Secondly, it is possible that galectin-3/ CD98 may change an integrin dimer conformation thereby affecting assembly of membrane bound adaptor molecules. Thirdly, galectin-3/ CD98 complex could affect the affinity of the receptor increasing the cell surface retention time of the integrin thereby increasing the fidelity of the signal. Finally, at a more conformational level, recognition of fibronectin bound to different surface topographies will result in surface dependent differences in the distribution of focal adhesions. Clustering of integrins in structurally different focal adhesions may result in differences in the availability of galectin-3 and CD98 to interact with their respective integrin and subsequently in the concentrations of membrane associated adaptor molecules thereby affecting the downstream signaling to the nucleus. This would be especially true if the galectin-3 were bound to β-galactoside containing lectin adsorbed to the cell surface.

5.7 Conclusion

The anisotropic etching of Si <110> crystals produced rough surfaces with tightly packed micro scale grooves. An advantage of the G1 and G2 surfaces over conventionally produced microgrooves surfaces is that they are easily produced in batch processes and do not require photolithography. The availability of novel micro scale substrata, such as G1 and G2, that produce distinctive profiles of macrophage secretions and behaviors provide new approaches to understanding the regulation of macrophage behavior that is important to the fate of implanted devices. In the absence of exogenously added cytokines or inflammatory mediators rough grooved surfaces appear to favor the development of a M2-like (wound healing) phenotype

probably through the formation of galectin-3/ CD98/ integrin β1 complex and downstream activation of PI3K. Blocking formation of the signaling complex also affected cell shape. It appears likely that substratum surface topography, which is in intimate contact with membrane components, influences formation of signaling complexes, their spatial environment and polarization of macrophage phenotype. Membrane components, such as β1-containing integrins, can therefore be added to the list of macrophage lineage-determining-cell-surface receptors.

5.8 Future Directions

1. For further investigation on the role of galectin-3 in regulating surface topography effects in RAW264.7 macrophages, galectin-3 or its membrane receptor CD98 can be deleted in RAW264.7 macrophages using small interfering RNA (siRNA) and expression of M1 and M2 markers and inflammatory cytokines can be measured at:
   a) The gene expression level by RT-qPCR
   b) The protein expression level by ELISA
2. Attachment of lactose to gal-3 can be measured using anti gal-3 antibody using western blot. Galectin-3 binds to lactose and the gal-3-lactose complex's molecular weight will be different from galectin-3 molecular weight.
3. Studying effects of lactose treatment on macrophages gene expression and cell morphology for a different time point (5 days or longer). As Ghrebi et al. (2013) has found that macrophage morphology changes over a 5-day period on smooth and rough topographies it would be interesting to study the effects of lactose treatment over longer times.

4. Studying effects of LY294002 treatment on macrophage cell morphology at the same or a different time point. LY294002 inhibits PI3K and its effect on macrophage morphology could be studied by confocal microscopy on smooth and rough topographies.

Bibliography

Abbas, A.K., Lichtman, A.H.H. & Pillai, S., 2014. Cellular and Molecular Immunology, Elsevier Health Sciences. 8th edition. p2,14,54.

Akira, S., Takeda, K. & Kaisho, T., 2001. Toll-like receptors: critical proteins linking innate and acquired immunity. *Nature Immunology*, 2(8), pp.675–680.

Anderson, J.M., Rodriguez, A. & Chang, D.T., 2008. Foreign body reaction to biomaterials. *Seminars in Immunology*, 20(2), pp.86–100.

Anderson, J.M., 1988. Inflammatory response to implants. *ASAIO Journal*, 34(2), pp.101–107.

Anderson, J.M. & Miller, K.M., 1984. Biomaterial biocompatibility and the macrophage. *Biomaterials*, 5(1), pp.5–10.

Baharloo, B., Textor, M. & Brunette, D.M., 2005. Substratum roughness alters the growth, area, and focal adhesions of epithelial cells, and their proximity to titanium surfaces. *Journal of Biomedical Materials Research. Part A*, 74(1), pp.12–22.

Barth, K. A, Waterfield, J.D. & Brunette, D.M., 2013. The effect of surface roughness on RAW 264.7 macrophage phenotype. *Journal of Biomedical Materials Research. Part A*, 101(9), pp.2679–88.

Berton, G. et al., 1994. Beta 2 integrin-dependent protein tyrosine phosphorylation and activation of the FGR protein tyrosine kinase in human neutrophils. *The Journal of cell biology*, 126(4), pp.1111–1121.

Berton, G. & Lowell, C. a, 1999. Integrin signalling in neutrophils and macrophages. *Cellular Signalling*, 11(9), pp.621–35.

Bogdan, C., 2001. Nitric oxide and the immune response. *Nature Immunology*, 2(10), pp.907–916.

Brandt, E. et al., 2000. IL-4 production by human polymorphonuclear neutrophils. *Journal of Leukocyte Biology*, 68(1), pp.125–130.

Brodbeck, W.G. et al., 2002. Biomaterial Surface Chemistry Dictates Adherent Monocyte/Macrophage Cytokine Expression *in Vitro*. *Cytokine*, 18(6), pp.311–319.

Brunette, D.M., 2001. Principles of cell behavior on titanium surfaces and their application to implanted devices. In *Titanium in Medicine*. Springer, pp. 485–512.

Buser, D., Broggini, N., Wieland, M., et al., 2004. Enhanced bone apposition to a chemically modified SLA titanium surface. *Journal of Dental Research*, 83(7), pp.529–533.

Bystry, R.S. et al., 2001. B cells and professional APCs recruit regulatory T cells via CCL4. *Nature Immunology*, 2(12), pp.1126–32.

Chehroudi, Babak, et al., 2010. Bone formation on rough, but not polished, subcutaneously implanted Ti surfaces is preceded by macrophage accumulation. *Journal of Biomedical Materials Research Part A* 93 (2), pp.724-737.

Chou, L. et al., 1998. Effects of titanium substratum and grooved surface topography on metalloproteinase‐2 expression in human fibroblasts. *Journal of Biomedical Materials Research*, 39(3), pp.437–445.

Chou, L. et al., 1995. Substratum surface topography alters cell shape and regulates fibronectin mRNA level, mRNA stability, secretion and assembly in human fibroblasts. *Journal of Cell Science*, 108(4), pp.1563–1573.

Chun, S.J., 2003. Integrin-linked kinase is required for laminin-2-induced oligodendrocyte cell spreading and CNS myelination. *The Journal of Cell Biology*, 163(2), pp.397–408.

Cooper, L.F., 2000. A role for surface topography in creating and maintaining bone at titanium endosseous implants. *The Journal of Prosthetic Dentistry*, 84(5), pp.522–534.

Cooper, L.F., 1998. Biologic determinants of bone formation for osseointegration: Clues for future clinical improvements. The Journal of Prosthetic Dentistry, (October), pp.439–449.

Curtis, A.S.G. & Wilkinson, C.D.W., 1998. Reactions of cells to topography. *Journal of Biomaterials Science, Polymer Edition*, 9(12), pp.1313–1329.

DiPrieto, L., et al., 1998. MIP-1 alpha as a critical macrophage chemoattractant in murine wound healing. *J. Clin. Investig* 10 (1), pp.1693-1698.

Dong, S. & Hughes, R.C., 1997. Macrophage surface glycoproteins binding to galectin-3 (Mac-2-antigen). *Glycoconjugate Journal*, 14(2), pp.267–274.

Dong, W.P., Sullivan, P.J. & Stout, K.J., 1994. Comprehensive study of parameters for characterising three- dimensional surface topography IV: Parameters for characterising spatial and hybrid properties. , 178, pp.45–60.

Edin, S. et al., 2013. Phenotypic skewing of macrophages in vitro by secreted factors from colorectal cancer cells. *PloS one*, 8(9), p.e74982.

Fukao, T. & Koyasu, S., 2003. PI3K and negative regulation of TLR signaling. *Trends in Immunology*, 24(7), pp.358–363.

García, A.J., 2005. Get a grip: integrins in cell-biomaterial interactions. *Biomaterials*, 26(36), pp.7525–9.

Ghrebi, S. et al., 2013. The effect of surface topography on cell shape and early ERK1/2 signaling in macrophages; linkage with FAK and Src. *Journal of Biomedical Materials Research Part A*, 101A(7), pp.2118–2128.

Goerdt, Sergij, and Constantin E. Orfanos., 1999. Other functions, other genes: alternative activation of antigen-presenting cells. *Immunity* 10 (2), pp.137-142.

Goldman, Robert D., 1971 The role of three cytoplasmic fibers in BHK-21 cell motility I. Microtubules and the effects of colchicine. *The Journal of Cell Biology* 51 (3), pp.752-762.

Gordon, S., 2003. Alternative activation of macrophages. *Nature Reviews Immunology*, 3(1), pp.23–35.

Gordon, S., 2007. The macrophage: past, present and future. *European Journal of Immunology*, 37 Suppl 1, pp.S9–17.

Groner, B. & Hennighausen, L., 2012. The versatile regulation of cellular events by Jak-Stat signaling: from transcriptional control to microtubule dynamics and energy metabolism. *Hormone Molecular Biology and Clinical Investigation*, 10(1), pp.193–200.

Le Guéhennec, L. et al., 2007. Surface treatments of titanium dental implants for rapid osseointegration. *Dental materials : official publication of the Academy of Dental Materials*, 23(7), pp.844–54.

Hamlet, S. et al., 2012. The effect of hydrophilic titanium surface modification on macrophage inflammatory cytokine gene expression. *Clinical Oral Implants Research*, 23(5), pp.584–90.

Henderson, N.C. et al., 2004. CD98hc (SLC3A2) interaction with beta 1 integrins is required for transformation. *The Journal of Biological Chemistry*, 279(52), pp.54731–41.

Henderson, N.C. & Sethi, T., 2009. The regulation of inflammation by galectin‐3. *Immunological Reviews*, 230(1), pp.160–171.

Holscher, C. et al., 2001. A Protective and Agonistic Function of IL-12p40 in Mycobacterial Infection. *The Journal of Immunology*, 167(12), pp.6957–6966.

Hong, H.L. & Brunette, D.M., 1978. Effect of cell shape on proteinase secretion by epithelial cells. , *Journal of Cell Science,* 87(2), pp. 259-267.

Hsu, D.K. et al., 2000. Targeted disruption of the galectin-3 gene results in attenuated peritoneal inflammatory responses. *The American Journal of Pathology*, 156(3), pp.1073–83.

Jiménez, C. et al., 2000. Role of the PI3K Regulatory Subunit in the Control of Actin Organization and Cell Migration. , *The Journal of Cell Biology*,151(2), pp.249–261.

Keegan, A.D. et al., 1995. Similarities and differences in signal transduction by interleukin 4 and interleukin 13 : Analysis of Janus kinase activation. , *Proceedings of the National Academy of Sciences*, 92(17), pp.7681–7685.

Kelly-welch, A.A.E. et al., 2003. Interleukin-4 and Interleukin-13 Signaling Maps Connections, *Science*,300(5625), pp.1527–1528.

Kreider, T. et al., 2007. Alternatively activated macrophages in helminth infections. *Current Opinion in Immunology*, 19(4), pp.448–53.

Lee, Sena J., et al., 2002. Mannose receptor-mediated regulation of serum glycoprotein homeostasis. *Science* 295 (5561), pp.1898-1901.

Legate, K.R. et al., 2005. ILK, PINCH and parvin: the tIPP of integrin signalling. *Nature Reviews Molecular Cell Biology*, 7(1), pp.20–31.

Legate, Kyle R., Sara A. Wickström, and Reinhard Fässler., 2009. Genetic and cell biological analysis of integrin outside-in signaling. *Genes & Development* 23 (4), pp.397-418.

Leonard, Warren J., and John J. O'Shea., 1998. Jaks and STATs: biological implications. *Annual Review of Immunology* 16 (1), pp.293-322.

Li, D. et al., 2002. Biomechanical comparison of the sandblasted and acid‐etched and the machined and acid‐etched titanium surface for dental implants. *Journal of Biomedical Materials Research*, 60(2), pp.325–332.

Linehan, Sheena A., Luisa Martínez-Pomares, and Siamon Gordon., 2000. Macrophage lectins in host defence. *Microbes and Infection* 2 (3), pp.279-288.

Liu, Fu-Tong, et al., 1995. Expression and function of galectin-3, a beta-galactoside-binding lectin, in human monocytes and macrophages. *The American Journal of Pathology* 147 (4), page.1016.

Loke, P'ng, et al., 2002. IL-4 dependent alternatively-activated macrophages have a distinctive in vivo gene expression phenotype. *BMC Immunology* 3 (1), page.7.

MacKinnon, A. C. et al., 2008. Regulation of Alternative Macrophage Activation by Galectin-3. *The Journal of Immunology*, 180(4), pp.2650–2658.

Mantovani, a et al., 2002. Macrophage polarization: tumor-associated macrophages as a paradigm for polarized M2 mononuclear phagocytes. *Trends in Immunology*, 23(11), pp.549–555.

Mantovani, A. et al., 2004. The chemokine system in diverse forms of macrophage activation and polarization. *Trends in Immunology*, 25(12), pp.677–86.

Martin, P. & Leibovich, S.J., 2005. Inflammatory cells during wound repair: the good, the bad and the ugly. *Trends in Cell Biology*, 15(11), pp.599–607.

Martinez, F.O., 2011. Regulators of macrophage activation. *European Journal of Immunology*, 41(6), pp.1531–1534.

Martinez, F.O. & Gordon, S., 2014. The M1 and M2 paradigm of macrophage activation: time for reassessment. *F1000prime reports*, 6(March), p.13.

McWhorter, F.Y. et al., 2013. Modulation of macrophage phenotype by cell shape. *Proceedings of the National Academy of Sciences*, 110(43), pp.17253–17258.

Meng, F. & Lowell, C. a, 1998. A beta 1 integrin signaling pathway involving Src-family kinases, Cbl and PI-3 kinase is required for macrophage spreading and migration. *The EMBO journal*, 17(15), pp.4391–403.

Meyle, J., Wolburg, H. & Von Recum, A.F., 1993. Surface micromorphology and cellular interactions. *Journal of Biomaterials Applications*, 7(4), pp.362–374.

Montecucco, F. et al., 2008. Tumor necrosis factor-alpha (TNF-alpha) induces integrin CD11b/CD18 (Mac-1) up-regulation and migration to the CC chemokine CCL3 (MIP-1alpha) on human neutrophils through defined signalling pathways. *Cellular Signalling*, 20(3), pp.557–68.

Morra, Marco., 2006. Biochemical modification of titanium surfaces: peptides and ECM proteins. *Eur Cell Mater* 12.1

Mosser, D.M., 2003. The many faces of macrophage activation. *Journal of Leukocyte Biology*, 73(2), pp.209–212.

Mosser, D.M. & Edwards, J.P., 2008. Exploring the full spectrum of macrophage activation. *Nature reviews. Immunology*, 8(12), pp.958–69.

Moy, F.J. et al., 2001. Solution structure of human IL-13 and implication for receptor binding. *Journal of Molecular Biology*, 310(1), pp.219–30.

Munder, M., Eichmann, K. & Modolell, M., 1998. Alternative Metabolic States in Murine Macrophages Reflected by the Nitric Oxide Synthase/Arginase Balance: Competitive Regulation by CD4+ T Cells Correlates with Th1/Th2 Phenotype. T*he Journal of Immunology,* 160(11), pp.5347–5354.

Nathan, C., 2012. Secretory products of macrophages: twenty-five years on. *The Journal of Clinical Investigation*, 122(4), pp.1189–90.

Nelms, K. et al., 1999. THE IL-4 RECEPTOR: Signaling Mechanisms and Biologic Functions. *Annual Review of Immunology*, 17(1), pp.701–738.

Nicolas, C.S. et al., 2012. The Jak/STAT pathway is involved in synaptic plasticity. *Neuron*, 73(2), pp.374–90.

O'Shea, J.J. & Murray, P.J., 2008. Cytokine signaling modules in inflammatory responses. *Immunity*, 28(4), pp.477–87.

Oakley, C. & Brunette, D.M., 1993. The sequence of alignment of microtubules , focal contacts and actin filaments in fibroblasts spreading on smooth and grooved titanium substrata. , *Journal of Cell Science,*106 (1), pp.343–354.

Oakley, C. & Brunette, D.M., 1995. Topographic compensation: guidance and directed locomotion of fibroblasts on grooved micromachined substrata in the absence of microtubules. *Cell Motility and The Cytoskeleton*, 31(1), pp.45–58.

Ozinsky, a et al., 2000. The repertoire for pattern recognition of pathogens by the innate immune system is defined by cooperation between toll-like receptors. *Proceedings of the National Academy of Sciences of the United States of America*, 97(25), pp.13766–71.

Perrin, D. et al., 2002. Bone response to alteration of surface topography and surface composition of sandblasted and acid etched (SLA) implants. *Clinical oral Implants Research*, 13(5), pp.465–469.

Puleo, D. A., and A. Nanci., 1999. Understanding and controlling the bone–implant interface. *Biomaterials* 20 (23), pp. 2311-2321.

Refai, A.K. et al., 2004. Effect of titanium surface topography on macrophage activation and secretion of proinflammatory cytokines and chemokines. *Journal of Biomedical Materials Research. Part A*, 70(2), pp.194–205.

Reizer, R., 2011. Simulation of 3D Gaussian surface topography. *Wear*, 271(3), pp.539–543.

Rich, A. K. H. A., and ALBERT K. Harris., 1981. Anomalous preferences of cultured macrophages for hydrophobic and roughened substrata. *Journal of Cell Science* 50 (1), pp. 1- 7.

Rintoul, R.C. et al., 2002. Cross-linking CD98 promotes integrin-like signaling and anchorage-independent growth. *Molecular Biology of The Cell*, 13(8), pp.2841–2852.

Russell, Stephen W., and Siamon Gordon, eds. 1992. Macrophage biology and activation. Springer Science & Business Media, page 24.

Satish L. Deshmane, Sergey Kremlev, Shohreh Amini, B.E.S., 2009. Monocyte Chemoattractant Protein-1 (MCP-1): An Overview. *Journal of Interferon and Cytokine Research*, 29(6), pp.313–326.

Sato, K. et al., 1998. Characterization of orientation-dependent etching properties of single-crystal silicon: effects of KOH concentration. *Sensors and Actuators A: Physical*, 64(1), pp.87–93.

Schmittgen, T.D. & Livak, K.J., 2008. Analyzing real-time PCR data by the comparative CT method. *Nature Protocols*, 3(6), pp.1101–1108.

Sica, A. et al., 2006. Tumour-associated macrophages are a distinct M2 polarised population promoting tumour progression: potential targets of anti-cancer therapy. *European Journal of Cancer,* 42(6), pp.717–27.

Sica, Antonio, and Alberto Mantovani., 2012. Macrophage plasticity and polarization: in vivo veritas. *The Journal of Clinical Investigation* 122.122 (3), pp.787-795.

Sittig, C., et al., 1999. Surface characterization. *Journal of Materials Science: Materials in Medicine* 10 (1), pp.35-46.

Solheim, Eirik, et al., 2000. Biocompatibility and effect on osteogenesis of poly (ortho ester) compared to poly (DL-lactic acid). *Journal of biomedical materials research* 49 (2), pp.257-263.

Spencer, Nicholas D., and John H. Moore., 2001. Encyclopedia of chemical physics and physical chemistry: Applications. Vol. 3. Taylor & Francis

Stanford, C.M., 2008. Surface modifications of dental implants. *Australian dental journal*, 53(1), pp.S26–33.

Stein, Michael, et al., 1992. Interleukin 4 potently enhances murine macrophage mannose receptor activity: a marker of alternative immunologic macrophage activation. *The Journal of Experimental Medicine* 176 (1), pp.287-292.

Szekanecz, Z. & Koch, A.E., 2007. Macrophages and their products in rheumatoid arthritis. *Current Opinion in Rheumatology*, 19(3), pp.289–295.

Takebe, J. et al., 2003. Titanium surface topography alters cell shape and modulates bone morphogenetic protein 2 expression in the J774A.1 macrophage cell line. *Journal of Biomedical Materials Research. Part A*, 64(2), pp.207–16.

Tan, K.S. et al., 2006. The role of titanium surface topography on J774A.1 macrophage inflammatory cytokines and nitric oxide production. *Biomaterials*, 27(30), pp.5170–7.

Textor, M. et al., 2001. Properties and biological significance of natural oxide films on titanium and its alloys. *Titanium in Medicine*. Springer, pp. 171–230.

Thompson, W.L. & Van Eldik, L.J., 2009. Inflammatory cytokines stimulate the chemokines CCL2/MCP-1 and CCL7/MCP-3 through NFkB and MAPK dependent pathways in rat astrocytes. *Brain Research*, 1287, pp.47–57.

Waterfield, J.D. et al., 2010. The effect of surface topography on early NFκB signaling in macrophages. *Journal of Biomedical Materials Research Part A*, 95A(3), pp.837–847.

Weiss, P., 1945. Experiments on cell and axon orientation in vitro: the role of colloidal exudates in tissue organization. *Journal of Experimental Zoology*, 100(3), pp.353–386.

Weisser, S.B. et al., 1998. Alternative Metabolic States in Murine Macrophages Reflected by the Nitric Oxide Synthase/Arginase Balance: Competitive Regulation by CD4 + T Cells Correlates with Th1/Th2 Phenotype. *European Journal of Immunology*, 41(6), pp.1742–53.

Wennerberg, A. & Albrektsson, T., 2009. Effects of titanium surface topography on bone integration: a systematic review. *Clinical Oral Implants Research*, 20 Suppl 4, pp.172–84.

Wennerberg, A., Albrektsson, T. & Lindhe, J., 2004. Surface topography of titanium implants. *Clinical periodontology and implant dentistry*.

Wieland, Marco. 1999. *Experimental determination and quantitative evaluation of the surface composition and topography of medical implant surfaces and their influence on osteoblastic cell-surface interactions*. Diss. Diss. Technische Wissenschaften ETH Zürich, Nr. 13247.

Wilson, H.M., 2014. SOCS Proteins in Macrophage Polarization and Function. *Frontiers in Immunology*, 5(July), p.357.

Wójciak-Stothard, Beata, et al., 1996. Guidance and activation of murine macrophages by nanometric scale topography. *Experimental cell research* 223 (2), pp.426-435.

Xagorari, Angeliki, and Katerina Chlichlia. 2008.Toll-like receptors and viruses: induction of innate antiviral immune responses." *The open microbiology journal* (2), page. 49.

Xia, Z. & Triffitt, J.T., 2006. A review on macrophage responses to biomaterials. *Biomedical Materials (Bristol, England)*, 1(1), pp.R1–9.

Zhang, X. & Mosser, D.M., 2008. Macrophage activation by endogenous danger signals. *The Journal of Pathology*, 214(2), pp.161–78.

Zhou, D. et al., 2014. Macrophage polarization and function with emphasis on the evolving roles of coordinated regulation of cellular signaling pathways. *Cellular Signalling*, 26(2), pp.192–7.

Appendix

Appendix A Supplemental Data

A.1 Effect of Lactose Treatment on Cell Number

RAW264.7 macrophages were cultured on polished surfaces and after 30 minutes 50mM lactose was added to their media. After 24 hours cells were observed using a phase contrast microscope and pictures were taken by a digital camera to observe any possible differences in the cell distribution between the control and lactose treated samples. In both control and treated samples cells were normally distributed on epoxy surfaces and no cell cluster or floating cells were observed in the presence of lactose.

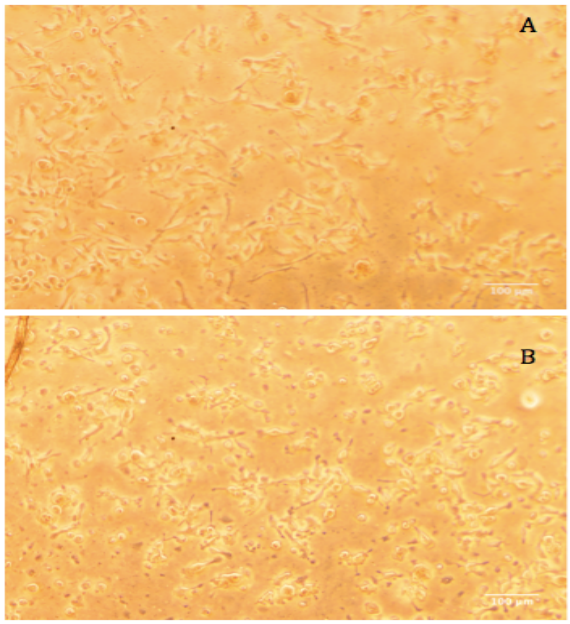

FigureA.1 Observing effects of lactose treatment on cell number in the presence (A) and absence (B) of lactose (50mM) using a Zeiss phase contrast microscope (Zeiss Canada Ltd) with a 10x magnification (day1). Pictures were taken by a Canon EOS D60 camera.

A.2 Number of cells on rough and smooth topographies in the presence and absence of lactose

Number of viable cells was measured on polished, SLA, G1 and G2 surfaces in the presence and absence of lactose after 24 hours following the cell culture by the MTS assay. There was no significant difference between cell numbers on smooth and rough topographies in the presence and absence of lactose.

A)

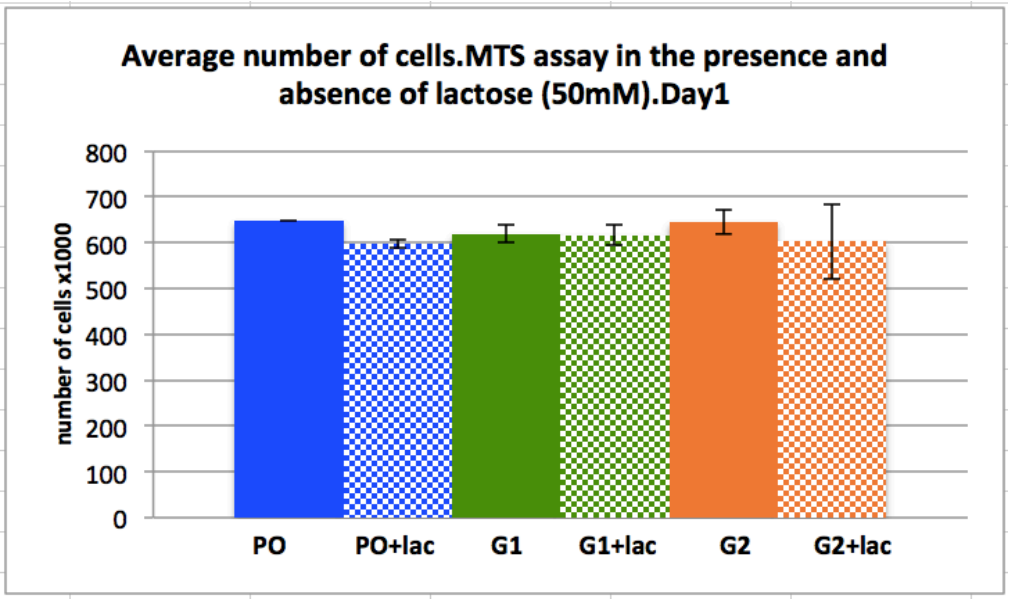

B)

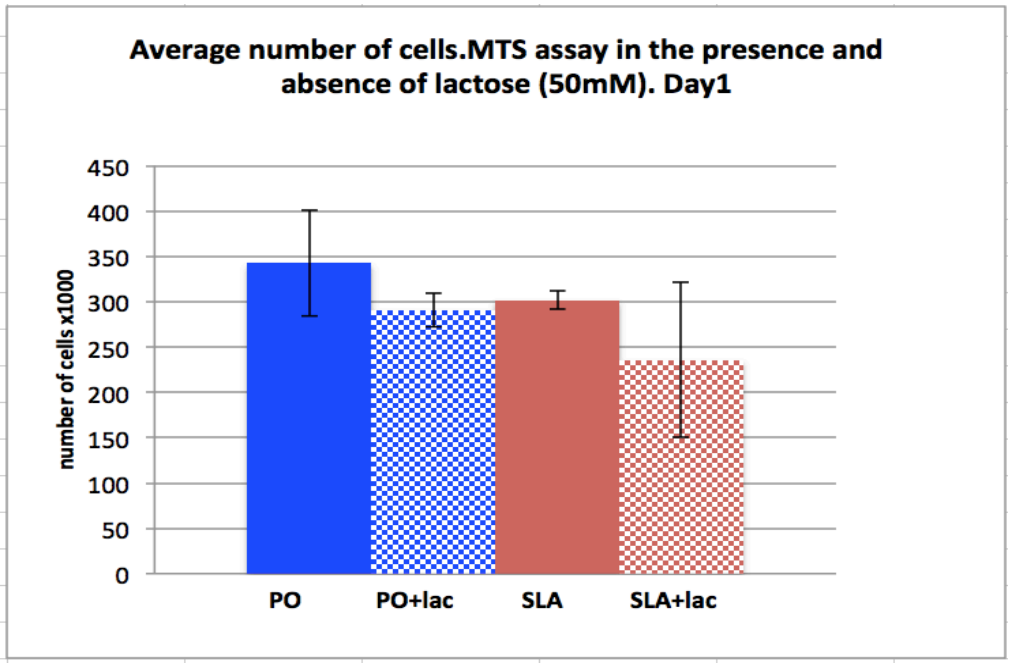

FigureA.2 Average number of RAW264.7 macrophage cells in the presence and absence of 50mM lactose on PO, SLA, G1 and G2 topographies (Day1). Initial number of cells seeded for day 1 was different for figure A and B. Error bars indicate standard deviation of 3 measurements.

A.3 Number of cells on rough and smooth topographies in the presence and absence of lactose measured by the MTS assay and DAPI staining

Number of cells was also counted manually on PO and G2 surfaces in the presence and absence of lactose (50mM) using DAPI staining and results were compared to the cell counting by the MTS assay. Stained macrophages with DAPI were observed under a UV-2E-C filter using an Axioscope 2 fluorescent microscope (Zeiss, Jena, Germany). As figure A.3 shows, similar to the results of the MTS assay, manually counting macrophages also shows that lactose treatment did not affect the cell number on smooth and rough surfaces.

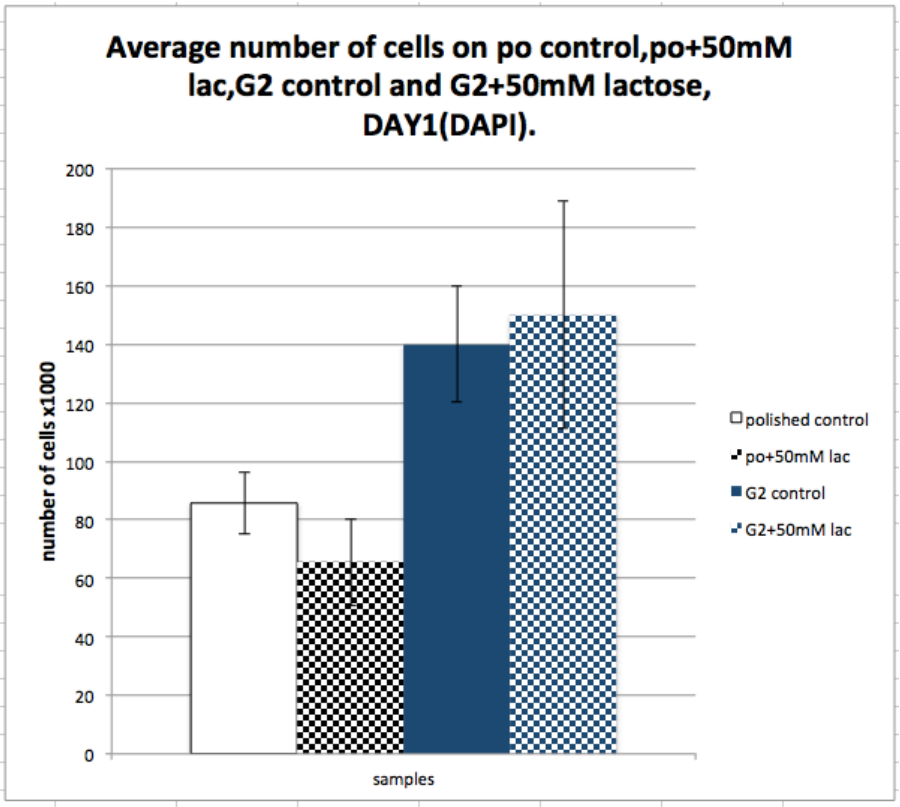

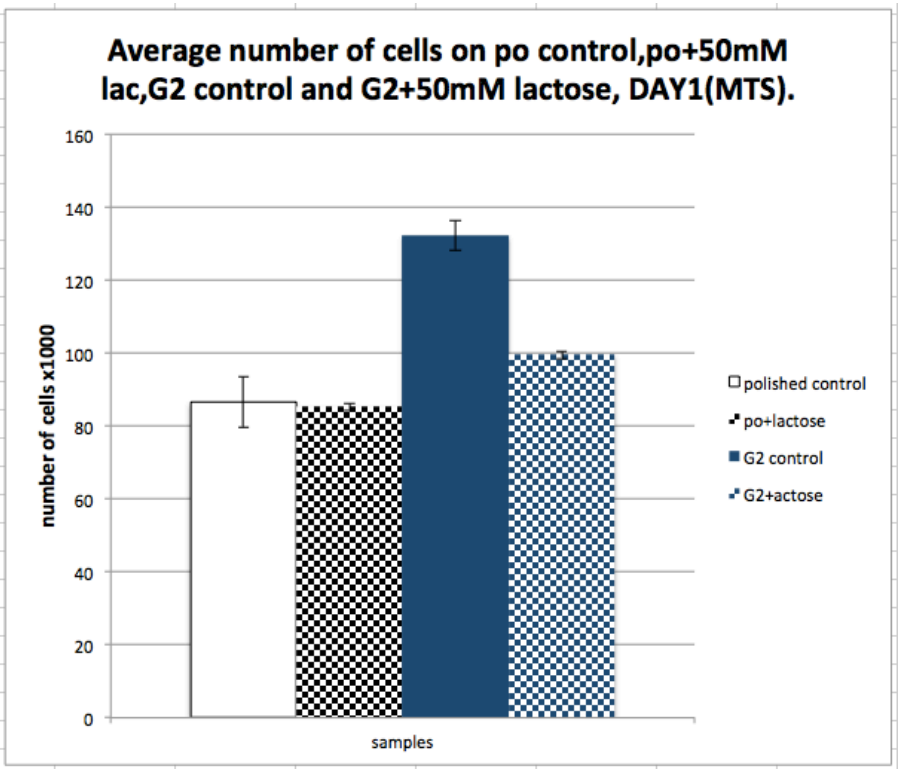

Figure A.3 Cell counting by MTS assay and DAPI staining on PO and G2 surfaces in the presence and absence of lactose (50mM) (Day1).

A.4 Average number of cells in the presence of IL-4 and LPS

Average number of viable cells on polished surfaces in the presence and absence of IL-4 (40ng/ml) and LPS (100ng/ml) was measured by MTS assay (Day1). Preliminary results show that cells were able to normally grow in the presence of IL-4 and LPS on the polished surfaces.

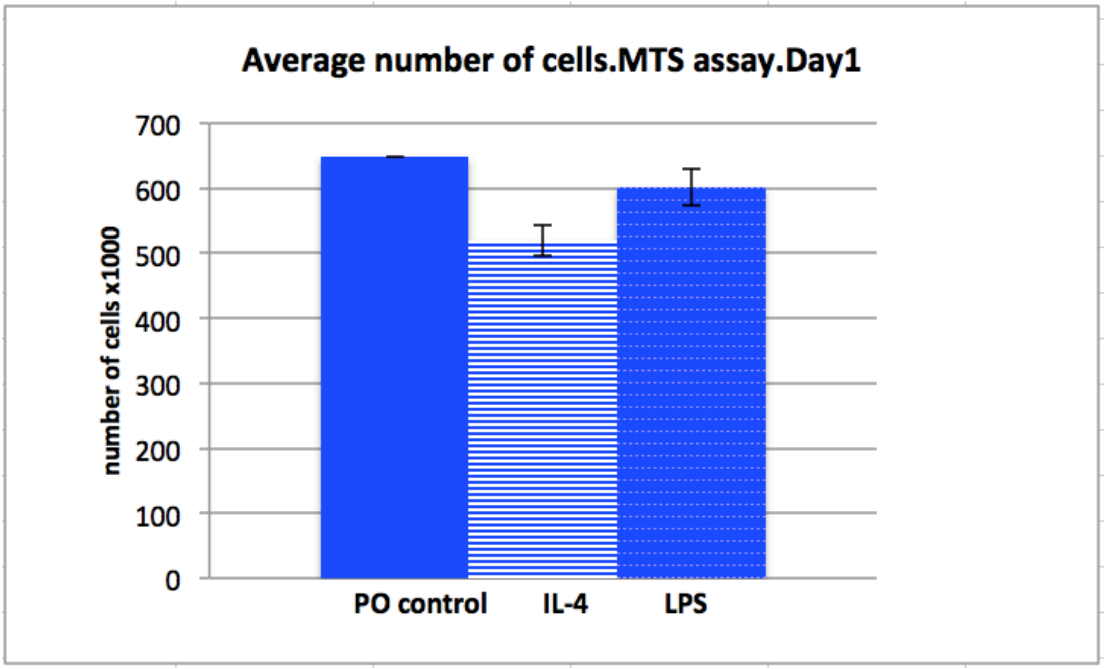

Figure A.4 Average number of RAW264.7 cells on polished surfaces in the presence and absence of IL-4 (40ng/ml) and LPS (100ng/ml) (Day1). Error bars indicate standard deviation of two measurements.

A.5 Cell number/ ml in the presence of DMSO (0.05%) on polished surfaces

Average number of viable cells on polished surfaces in the presence and absence of DMSO was measured by MTS assay (Day1). DMSO treatment had no significant effect on the number of cells on the polished surfaces.

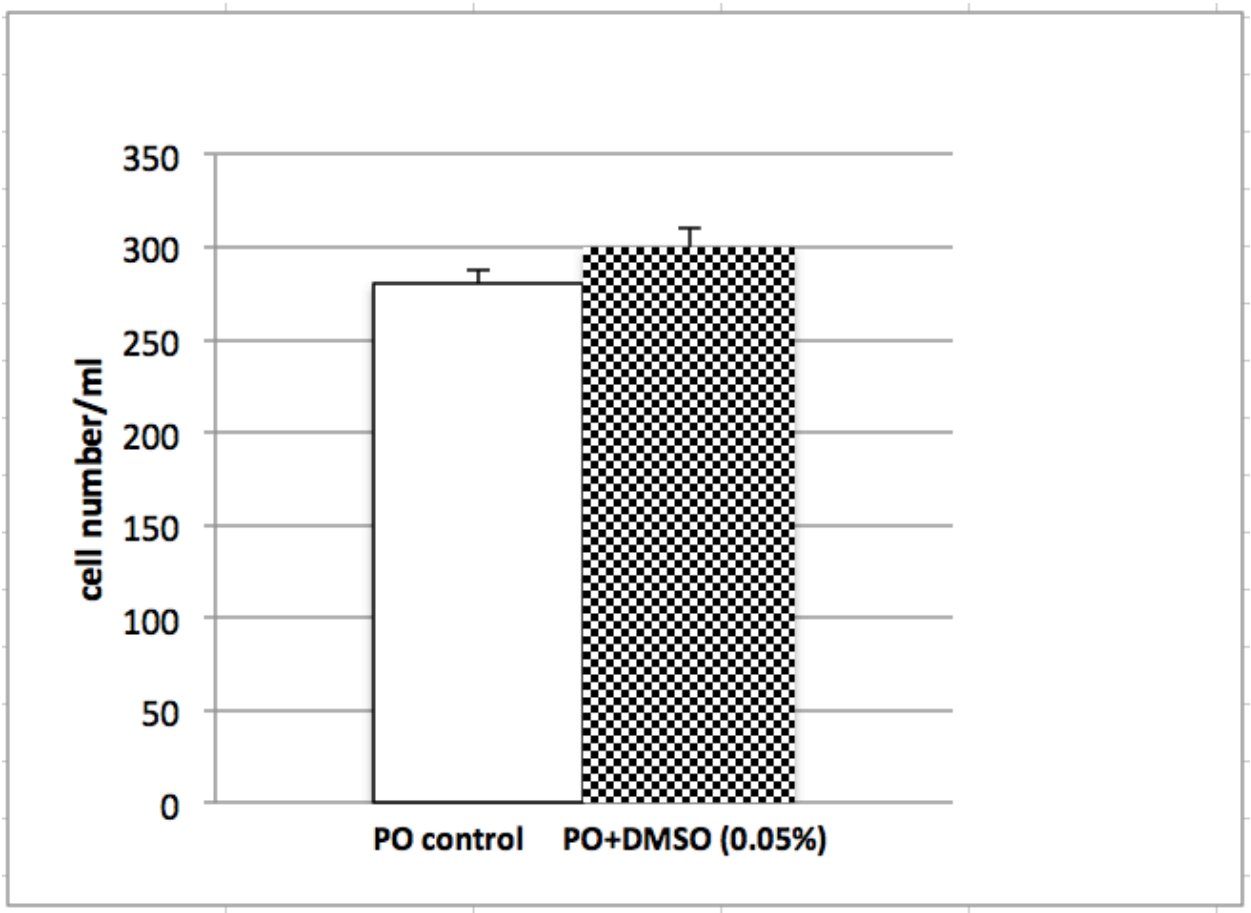

Figure A.5 Average number of RAW264.7 cells on polished surfaces in the presence and absence of DMSO (Day1). Error bars indicate standard deviation of two measurements.

A.6 Cytokine Microarray

Expression of IFN, IL-10, IP-10, CCL2, CCL3, CCL4, CXCL2, TNF, IL-1, IL-1r and IL-23 was measured on polished, G1 and G2 surfaces in the presence and absence of lactose (50mM) after day1. Preliminary results showed that among all cytokines, CCL3 had higher expression on G1 and G2 surfaces in the presence of lactose after 24 hours.

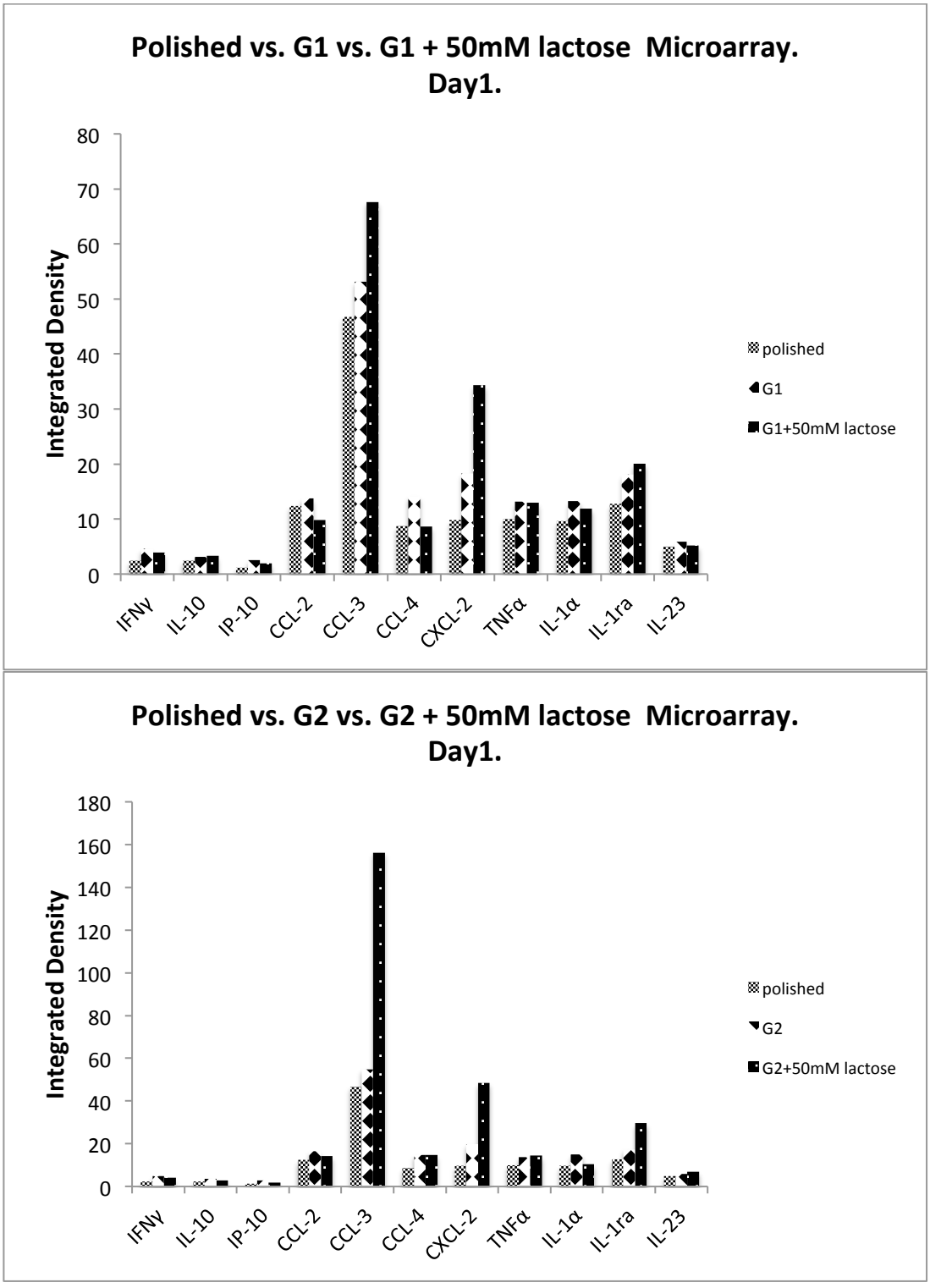

Figure A.6 Cytokine microarray results of RAW264.7 macrophage cultured on PO, G1 and G2 surfaces in the presence and absence of lactose (Day1).

A.7 CCL3 ELISA Results

As higher expression for CCL3 was detected by cytokine microarray on G1 and G2 surfaces in the presence of lactose, expression of CCL3 was also measured by ELISA on polished, G1 and G2 surfaces in the presence and absence of lactose (Day1). Preliminary results show that CCL3 was upregulated in the presence of lactose on G2 surfaces after 24 hours, however, when the experiment was repeated (with the same experiment setting; SLA was included) there was a little difference between the expression of CCL3 on G2 surfaces in the presence and absence of lactose. More experiments are needed.

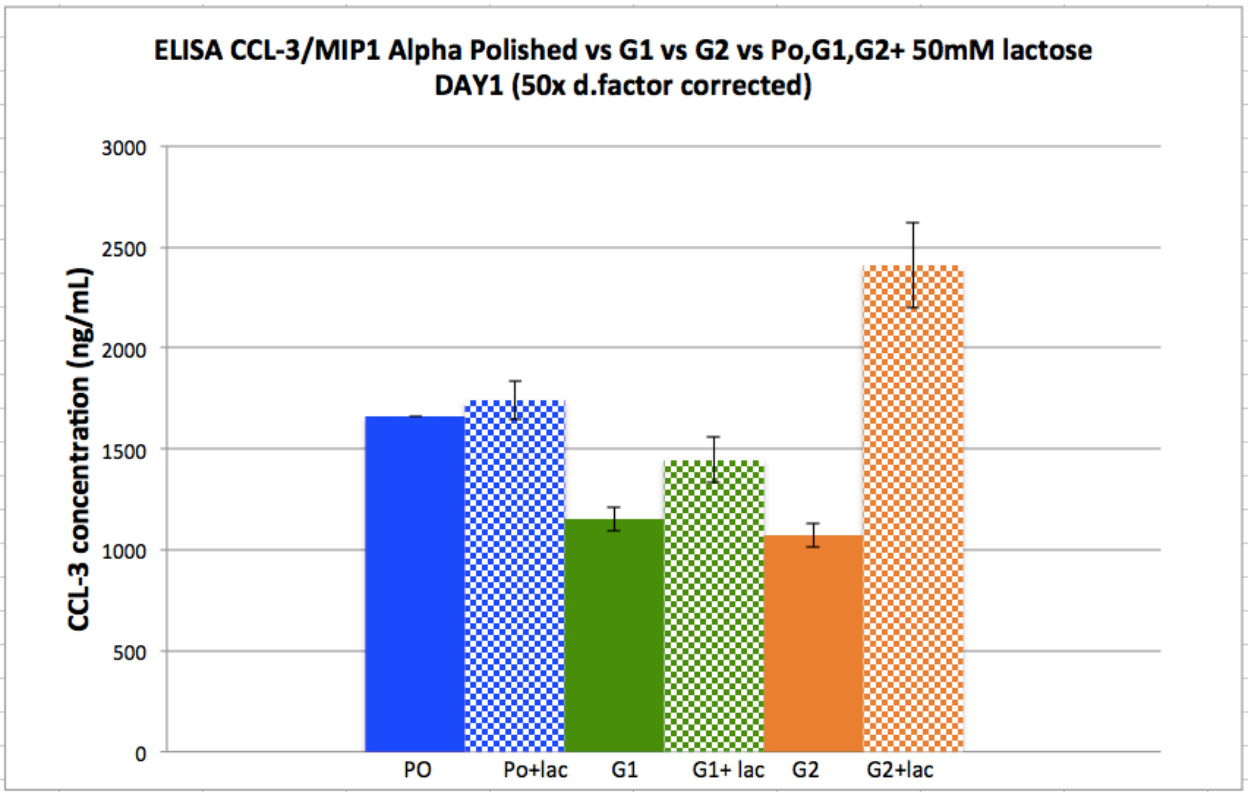

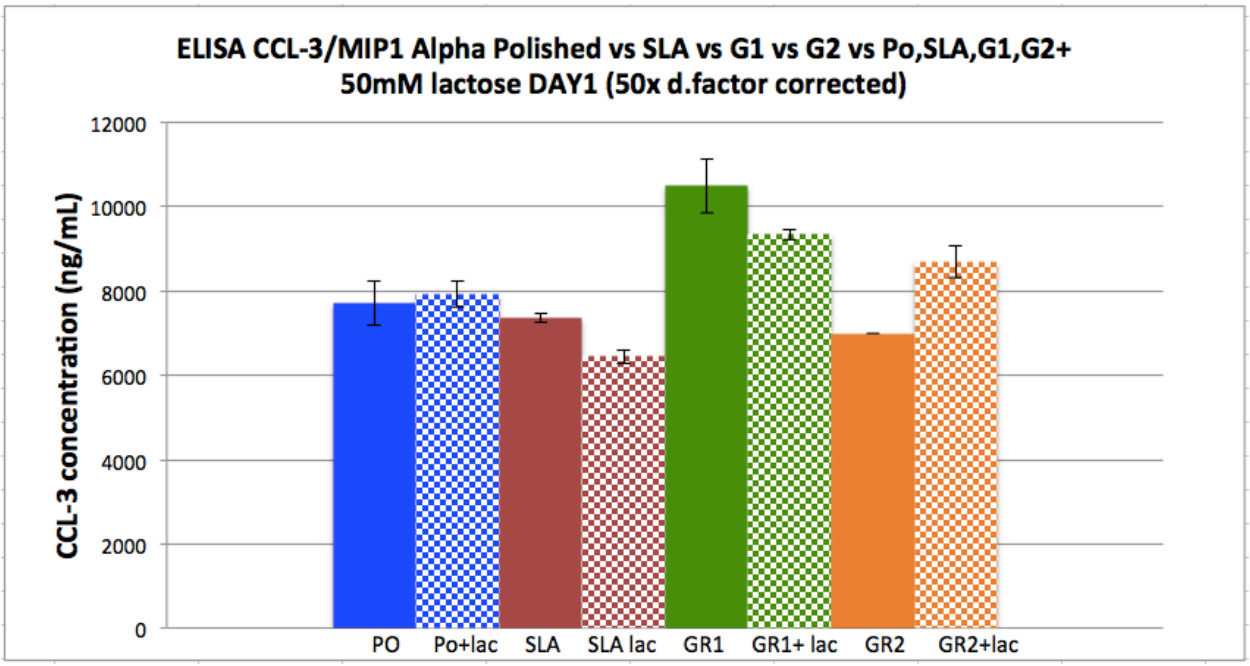

Figure A.7 CCL3 expression on PO, SLA, G1 and G2 surfaces in the presence and absence of lactose measured by ELISA (Day1). Error bars indicate standard deviation of three measurements.

A.8 CCL3 ELISA Results

As CCL3 is a macrophage inflammatory protein, expression of CCL3 was measured in the presence and absence of LPS (inflammatory phenotype inducer) on polished surfaces (Day1). CCL3 expression was highly upregulated on PO surfaces in the presence of LPS.

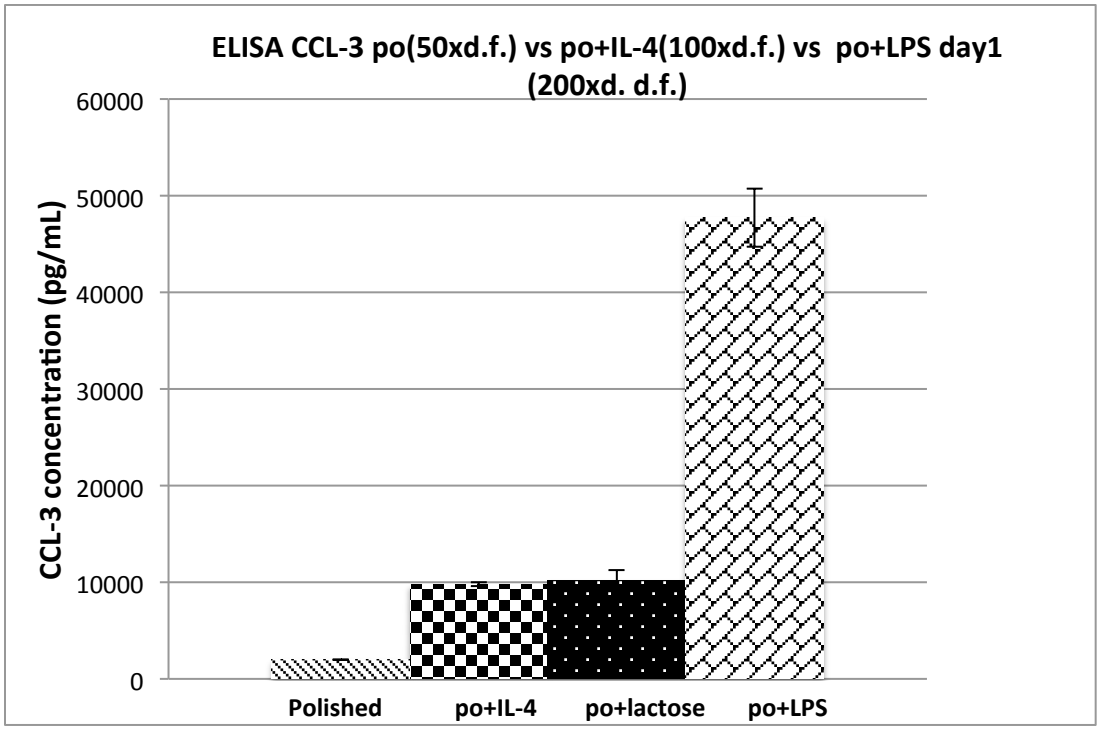

Figure A.8 CCL3 expression on PO surfaces in the presence and absence of IL-4 (40ng/ml), lactose and LPS (100ng/ml) measured by ELISA (Day1). Error bars indicate standard deviation of three measurements.